Planetary rings

To cite this article: Larry W Esposito 2002 *Rep. Prog. Phys.* **65** 1741

INSTITUTE OF PHYSICS PUBLISHING REPORTS ON PROGRESS IN PHYSICS

Rep. Prog. Phys. **65** (2002) 1741–1783 PII: S0034-4885(02)88971-0

Planetary rings

Larry W Esposito

LASP, University of Colorado, 392 UCB Boulder, CO 80309-0392, USA

Received 19 February 2002, in final form 21 August 2002
Published 12 November 2002
Online at stacks.iop.org/RoPP/65/1741

Abstract

In our solar system, planetary rings are found around all the giant planets, showing spectacular variety. Jupiter's thin ring system is composed mostly of dust. Saturn's rings are the largest and best studied, and the target of the NASA/ESA Cassini space mission that will begin orbiting Saturn in 2004. Its ring system consists of the broad A and B rings (separated by the Cassini Division) and the optically thinner C and D rings. Outside the main rings are the narrow 'braided' F ring and rings E and G. Uranus has ten narrow, sometimes eccentric rings and a family of dust bands. Neptune has three distinct rings (Galle, LeVervier, and Adams); the outermost Adams ring is patchy, with the thicker segments termed 'arcs.' All the ring systems have moons interspersed, which sculpt, collect, and release ring material. Moons are the likely parents of the present rings, ground down by meteorites and destroyed randomly to produce the relatively short-lived ring systems. Thus, we observe the natural stochastic results of birth and death processes when we examine the rings closely. Ring systems are relatively nearby and provide a natural laboratory for phenomena in flattened disks, including the nebula around our Sun that gave rise to the planets. Cassini will observe Saturn's rings and the numerous physical phenomena occurring within them close-up from 2004 to 2008, refining and possibly redefining our view of ring physics.

Contents

1. Introduction: the allure of the ringed planets

One of the most enduring symbols of space exploration is a planet surrounded by a ring. This symbol inspires a celestial context: nothing on Earth is like it. My own fascination with space began when first I saw Saturn and its rings through a small telescope. The study of planets and rings has become my lifelong vocation, or perhaps addiction. What a wonderful surprise that the ringed planets are just as beautiful and scientifically compelling seen close-up! Furthermore, the ringed planets are not just objects of beauty, but complicated physical systems that provide a local laboratory and analogy for other flat systems like galaxies and planet-forming disks.

We now know that planetary rings, once thought unique to the planet Saturn, exist around all the giant planets. These rings are not solid objects, but composed of countless particles with sizes from specks of dust to small moons. For each planet, the rings are quite different. Jupiter's ring is thin and composed of dustlike small particles. Saturn's rings are broad, bright, and opaque. Uranus has narrow, dark rings among broad lanes of dust that are invisible from Earth. Neptune's rings include incomplete arcs restricted to a small range of their circumference. All rings lie predominantly within their planet's Roche limit, where tidal forces would destroy a self-gravitating fluid body. They are also within the planet's magnetosphere, and in the case of Uranus, they are within the upper reaches of the planetary atmosphere.

The common occurrence of ring material around the planets is one of the major scientific findings of the last twenty-five years. The new ring systems were discovered by both spacecraft and ground-based observers, often surprising us by contradicting our expectations. The rings' appearance and their composition vary among the various planets, and likewise within each ring system. The broadest set of rings and the most identified processes are found around the planet Saturn, which is the target of the US/European Cassini space mission to arrive in 2004.

The detailed views from spacecraft, ground telescopes, and Hubble show the following structural features in planetary rings: vertical thickness considerably greater than the average particle size; dark lanes, gaps, and other density variations; eccentric and inclined rings; sharp edges; azimuthal brightness variations, arcs and clumps; waves and wakes; and incomplete, kinked, and apparently braided rings. We still lack good explanations for much of this dazzling variety of phenomena, although many of these features have been explained by gravitational interactions between the ring particles and nearby moons.

Beyond the interactions with moons (many of which were likewise discovered by close-up pictures from spacecraft), the ring particles interact with the planet's magnetosphere via charging, plasma drag, and forces from the planet's own magnetic and electric field. Electrostatic effects lift small particles from the surface of the larger ring particles to create the dark radial lanes, called spokes, that are seen in the Voyager Saturn pictures. Ring particles suffer a gas drag from the extended planetary atmosphere that causes them to spiral inwards to destruction.

Ring particles come in a broad range of sizes. Their size distribution extends from submicron dust, through metre-sized particles, to small embedded moons like Saturn's moon Pan, about 10 km in radius. Perhaps 100–1000 moons larger than 1 km orbit each of the giant planets but were too small to be detected by spacecraft cameras. Theoretical expectations and some data support the idea that the particles in a ring will segregate in size, both radially and vertically.

What are ring particles made of? The ring composition is well known only for Saturn. Spectroscopic, occultation, and neutron measurements all imply that Saturn's rings particles are almost entirely water ice and bright like the surfaces of Saturn's inner satellites. For the other ring systems, the particles resemble the nearby small moons and probably contain significant silicate, and in the case of Uranus and Neptune, possible carbonaceous material. Even in the Saturn rings, colour variations may indicate compositional differences between different parts of the rings.

Radio occultations at two wavelengths have provided size information for the Saturn and Uranus rings (unfortunately excluding Saturn's B ring because of its opacity) in the range of roughly 1 cm to 10 m. Information on smaller particles is from photometry and differential opacity in stellar occultations. The derived size distributions are broad power-law distributions, with power-law index around three. These distributions are similar to those arising from catastrophic fragmentation of small solid bodies.

We have a first-order understanding of the dynamics and key processes in rings, much of it based on previous work in galactic and stellar dynamics. The rings are a kinetic system, where the deviations from perfect circular, equatorial motion can often be considered as random velocities in a viscous fluid. Unfortunately, the models are often idealized (for example, treating all particles as hard spheres of the same size) and cannot yet predict many phenomena in the detail observed by spacecraft (for example, sharp edges). Non-intuitive collective effects give rise to unusual structures.

The rings show many youthful features: Saturn's ice is bright and undarkened by meteoritic dust, the Uranus rings are narrow, Neptune's arcs are constrained to a small range of longitude, and Jupiter's ring particles are so small that they will be dragged away into the planet's atmosphere in a thousand years or less. The angular momentum that is now being transferred between rings and the nearby moons through density waves should have caused them to spread much further apart than they currently are. Further, the small moons discovered by Voyager could not themselves have survived the flux of interplanetary meteoroids for the age of the solar system. In much less time, these small moons would certainly be shattered by an impacting object. This realization provides a potential solution to the problem of young rings. These impacts not only destroy the moons, they can also recreate the ring systems! The new rings would gradually spread and eventually be ground to dust. Thus, the moons not only sculpt the rings' structure; they also provide the reservoirs for past and future ring systems.

I will emphasize that most rings are much younger than the solar system and the likely explanation that new rings are episodically created by the destruction of small moons near the planets. This idea is one example of how recent spacecraft observations have shown a larger role for catastrophic events in the history of the solar system. The role of giant impacts seems essential in explaining the history of planetary rings, along with the origin of the Earth's moon, the history of life on Earth, the rotation and tilt of the planets, and the unique aspects of both Mercury and Pluto. Thus, the study of rings connects with the interest in similar processes in the formation of the Earth's moon and the question of the demise of the dinosaurs.

This unexpected range of phenomena seen in planetary rings gives some insight into the processes in other flattened astrophysical systems. The processes observed now in planetary ring systems parallel those that occurred at the time of the origin of the planets. Clearly, the rings are not now accreting to form planets, as the original planetesimals did. However, many processes are occurring now in rings that resemble those in the solar nebula, particularly interactions between the disk and embedded objects. Models of the present processes in rings can be compared in detail to ring observations, allowing testing and refinement that is no longer possible for the early solar system.

This review briefly describes the rings in the solar system and some mathematical and physical approaches to understanding them. I will emphasize the variety of ring phenomena revealed in the last two decades from space and Earth observations. I address in some detail the recent history of rings and conclude with a discussion of the major open questions and future opportunities to learn about planetary rings. This paper benefits from previous reviews by Esposito *et al* (1984, 1991), Esposito (1986, 1993), Nicholson and Dones (1991), Cuzzi (1995, 1998), Porco *et al* (1995), and Burns *et al* (2001).

2. Diversity of planetary rings

Planetary rings are composed of myriad small particles, mostly orbiting inside the Roche limit of the giant planets. The *Roche limit* is the distance closer than which a fluid particle would be disrupted by tidal forces from the planet; at this limiting distance, the tides are just balanced by the self-gravity of the object (Weidenschilling *et al* 1984). An interesting exercise is to compare all the ring systems when normalized to the equatorial radius of each planet (see figure 1, after Nicholson and Dones (1991)). This comparison clearly shows that the rings occupy a common location near the planets, overlapping with numerous small moons (called *ringmoons*) near the rings (Thomas 1989). As we shall see, these moons are dynamically (and, likely, genetically) related to the nearby rings.

The properties of the individual particles in the rings are poorly known. We have the best information for Saturn's rings, which are the brightest and have been studied from the ground since their discovery by Galileo in 1610 (see, e.g. van Helden (1984)). Our current understanding is summarized in table 1 (Nicholson and Dones 1991, Burns *et al* 2001).

3. Large-scale ring physics

3.1. Particle dynamics

The first modern step towards understanding planetary rings was made just before the discovery of the Uranus rings in 1977 through the study of simple unperturbed collisional systems. The collisional dynamics of a differentially rotating disk of particles have been studied extensively (see, e.g. Lynden-Bell and Pringle (1974), Brahic (1975, 1977), Goldreich and Tremaine (1978), and Lin and Papaloizou (1979)). The main results can be summarized as follows (Brahic 1977): after a very fast flattening within a time of the order of a few tens of collisions per particle, the system reaches a quasi-equilibrium state in which the thickness of the newly formed disk is finite (i.e. the centres of the particles do not lie in the same plane) and in which collisions still occur. Under the combined effect of differential rotation and inelastic collisions, the disk spreads very slowly; particles move both inwards and outwards carrying some angular momentum while conserving the total angular momentum of the system. In the absence of external confining forces, the spreading time is of the order of the time it takes particles to execute a random walk of a distance equal to the ring width. During particle collisions, part of the relative velocity arising from differential rotation is transformed into vertical and radial motion. A steady state is established between this kinetic energy received by the system from differential rotation and that drained away through inelastic collisions, so that the kinetic energy that is continually lost by individual particles is obtained at the expense of potential energy from the bodies moving inwards and outwards. Because angular momentum is conserved, the energy lost by the inward motion of a portion of the particles is larger than the energy gained by the remainder that are moving outwards: to spread, the disk gives up a small amount of its total energy.

The first analytical studies of ring dynamics solved the Boltzmann equation with a specified collision integral on the right-hand side. In order to solve this equation, Goldreich and Tremaine (1978a, 1982), Araki and Tremaine (1986), Shu and Stewart (1985), and Hammeen-Anttila (1978) have introduced simplifications to the complete Boltzmann equation based on several assumptions. An important question is to relate the numerical results to real rings. Rather than

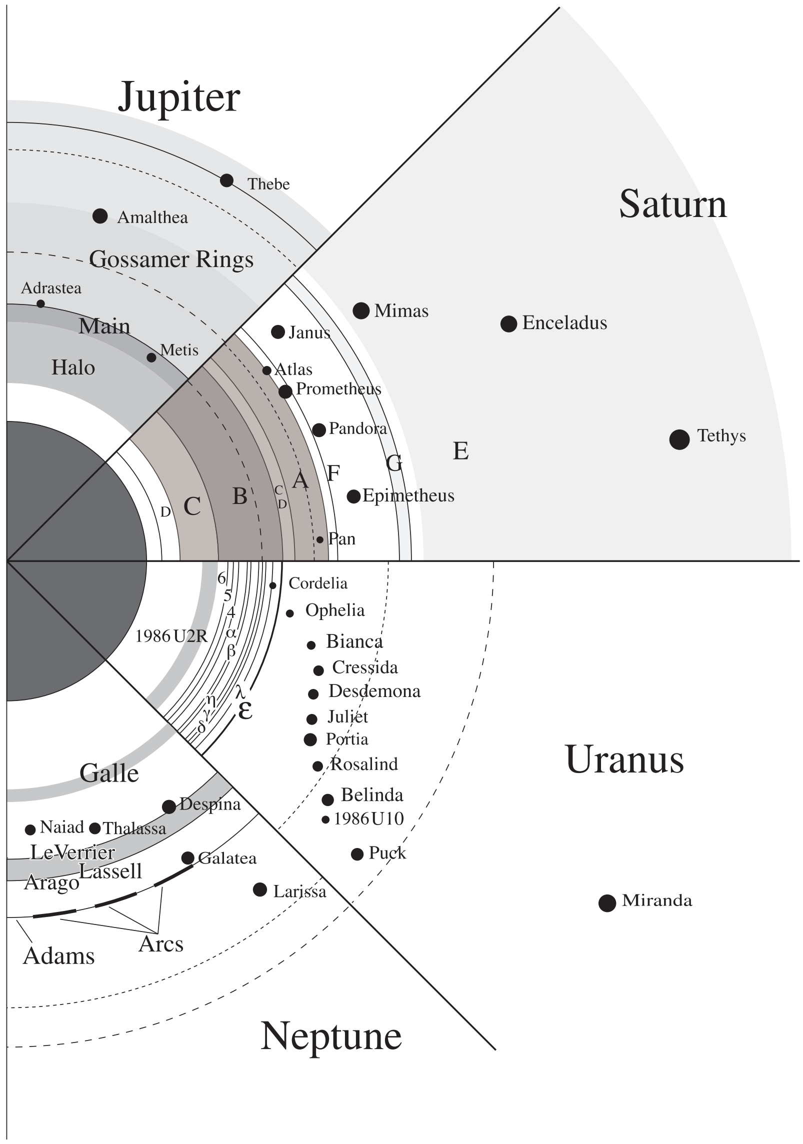

Figure 1. A comparison of the four planetary ring systems, including the nearby satellites, scaled to a common planetary equatorial radius. Density of crosshatching indicates the relative optical depth of the different ring components. Synchronous orbit is indicated by a dashed line, the Roche limit for a density of 1 gm cm^{-3} by a dot-dash line. Figure courtesy of Judith K Burns, from Burns *et al* 2001 Dusty rings and circumplanetary dust pp 641–725 *Interplanetary Dust* ed E Grun, B A S Gustafson, S F Dermott and H Fechtig, © 2001 Springer-Verlag, reproduced by permission of the publisher.

trying to reproduce any particular observed feature, these studies have served to investigate the important physical mechanisms. More modern research has used N-body simulations to explicate the phenomena (see, e.g. Salo (1995), Salo and Hänninen (1998), Lewis and Stewart (2000), Lewis (2001)). Lewis and Stewart (2000) show that the ring dynamics are significantly more complex than a standard fluid model, due to the actual sizes of particles and alignment of particle epicyclic phases.

Table 1. Planetary rings characteristics.

	Location (width)	Optical depth	Dust fraction (%)	Power-law index	Notes
			Jupiter		
Halo	92 000–122 500	10^{-6}	100	?	12 500 km thick
Main ring	122 000–128 980	3×10^{-6}	~50 (?)	$q \leqslant 2.5$	Bounded by Adrastea
Almalthea Gossamer	129 000–182 000	10^{-7}	100 (?)	?	2000 km thick
Thebe Gossamer	129 000–226 000	3×10^{-8}	100 (?)	?	4400 km thick
			Saturn		
D ring	66 000–74 000	10^{-3}	50 100	?	Internal structure
C ring	74 490–91 983		<3	3.1	Some isolated ringlets
B ring	91 983–117 516	$\leqslant 2.5$	<3	2.75	Abundant structure
Cassini Division	117 516–122 53	0.05–0.15	<3		Several plateaus
A ring	122 053–136 774	~	<3	2.75–2.90	Many density waves
F ring	140 200 ($W \cong 50$ km)	0.1–0.5	>98	2–3	Narrow, broad components
G ring	166 000–173 000	10^{-6}	>99	1.5–3.5	
E ring	180 000–450 000	10^{-5}	100		Peak near Enceladus
			Uranus		
1986 U2R	37 000–39 500	10^{-4}–10^{-3}	?	?	Still unnamed
Dust belts	41 000–50 000	10–5	?	?	Fine internal structure
6	41 837	0.3	<1%	$q > 3.5$	
5	42 234	0.5	<1%	$q > 3.5$	
4	42 570	0.3	<1%	$q > 3.5$	
α	44 718	0.3	<1%	$q > 3.5$	
β	45 661	0.2	<1%	$q > 3.5$	
η	47 175	0.3	<1%	?	
λ	50 023	10^{-3}	>95	?	
γ	47 627	2	<1%	?	
δ	48 300	0.4	<1%	?	
ε	51 149	0.5–2.3	<1%	$2.5 < q < 3.0$	Adjacent to Cordelia
			Neptune		
Galle	41 000–43 000	$4\text{–}10 \times 10^{-5}$	?	?	
LeVervier	53 000 ($W = 10$ km)	10^{-2}	40–70	?	Adjacent to Despina
Lasell	53 000–58 000	$1\text{–}3 \times 10^{-4}$	?	?	
Adams	62 930 ($W = 50$ km)	10^{-2}	20–50	?	Adjacent to Galatea
Adams arcs	62 930 ($W = 10$ km)	10^{-1}	40–70	?	

Sources: Burns *et al* (2001), Nicholson and Dones (1991), French *et al* (1991).

3.2. Mechanisms for ring confinement

A significant mechanism for confining rings has been quantitatively studied by Goldreich and Tremaine (1978b, 1979, 1982). Through gravity, a nearby satellite will alter a ring particle's orbit, making it elliptical. This effect is especially pronounced where the period of the ring-particle orbit is in the ratio of small integers to the period of the perturbing satellite. Such a location is termed a *resonance* and labelled by the ratio of periods; i.e. at the

'Mimas 2 : 1 resonance,' a ring particle orbits Saturn twice each time Mimas orbits once. The overall effect of the resonant perturbations on a population of particles in a disk is to increase the density of particles in some places and to decrease it in other places; this pattern is static in the satellite's frame but moves through the disk and thereby generates spiral density waves like those in spiral galaxies (compare with Shu (1970)). If the perturbing satellite is exterior to the ring, this wave moves outwards from the resonance, carrying negative energy and negative angular momentum. An isolated ring particle would not suffer any systematic drift after the encounter with the satellite (although its subsequent motion is complicated). Because rings are dense enough to have numerous collisions between particles, the particles involved in such collisions gradually move inwards towards the planet. In other words, encounters with a satellite increase radial motions, while collisions circularize the orbits. A balance is achieved in which the particle orbits accommodate to the perturbing influence (Brophy *et al* 1992). The net effect is thus a repulsion of the orbits due to the gravitational attraction between the ring and moon (see Greenberg (1983))! Cuzzi (1998) compares this *shepherding* to an overly protective parent who ends up repelling rather than attracting his children. The exterior satellite removes angular momentum from the ring and adds energy to nearby particles, thus transferring angular momentum from the ring to its orbit (see, e.g. Lin and Papaloizou (1979)). If the angular momentum luminosity carried off by this wave exceeds that carried by the particles diffusing across the resonance, the wave truncates the ring and an edge is formed (Goldreich and Tremaine 1979). An example is provided by the Uranus system, where known satellites (for the ε ring) as well as small undetected satellites (for the other rings) on each side of a narrow ring can thus constrain its edges and prevent the ring from spreading. Elliptical and inclined rings can also be generated by such a confining mechanism (Goldreich and Tremaine 1982).

The precise mechanism for shepherding has not been completely determined (Borderies *et al* 1989, Brophy *et al* 1990, Lewis and Stewart 2000, Lewis 2001) but can be qualitatively understood as follows. Satellites exert torques on the boundary of a ring located at a low-order resonance. For the simplest case of a circular ring and a circular satellite orbit, the strongest torques occur where the ratio of the satellite orbit period to the ring-particle period equals $m/(m+1)$ with m an integer. The torque is of the order of

$$T_m = \frac{\pm m^2(G^2 m_s^2 \sigma)}{\Omega^2 r^2} \tag{1}$$

(Goldreich and Tremaine 1980). G, Ω, m_s, r, and σ are, respectively, the gravitational constant, the orbital frequency, the satellite mass, the orbital radius, and the surface mass density evaluated at the resonance location. If the spacing between neighbouring resonances from a nearby satellite is very small, the widths of individual resonances can be greater than the separations, so that resonances overlap. Thus, it is useful to sum the discrete resonance torques and to define the total torque on a narrow ringlet of width Δr:

$$T \sim \frac{\pm(G^2 m_s^2 \sigma r \Delta r)}{\Omega^2 x^4} \tag{2}$$

where x is the separation between the satellite and the ringlet ($r \gg x \gg \Delta r$) (Goldreich and Tremaine 1980).

The presence of dissipation is essential, since the torque would vanish without it. In that case, the nearby moon has no long-term effect on the ring. The exact nature of the dissipation does not affect the expression of the torque (Greenberg 1983, Meyer-Vernet and Sicardy 1984), as suggested by the fact that the torque expression does not explicitly contain any dependence on dissipation. Particle collisions are evidently the main source of dissipation. The physics involving many colliding particles sets the study of ring dynamics apart from classical celestial dynamics, in which no collisions are assumed, and fluid dynamics, in which more frequent collisions are known to occur than in planetary rings (where the mean free path of an individual particle may be much longer than in the fluid case). Further, because each ring particle is on an individual orbit, unlimited separations are impossible.

Note that the resonance torque would not act on isolated test particles. For example, due to the rarity of collisions in the asteroid belt, this mechanism is not responsible for the formation of the Kirkwood gaps. Instead, chaotic motion of asteroids excited by Jupiter depopulates this region and may bring meteorites to Earth.

The rate of transfer of angular momentum can also be calculated by a perturbative approach without reference to individual resonances. The gravitational interaction of a ring particle with a satellite occurs primarily close to encounter. Their relative motion is not perfectly symmetric around encounter, so that the tangential component of the relative velocity of the particle with respect to the satellite is reduced, and thus angular momentum is exchanged with the net result that the ring experiences a torque (Lin and Papaloizou 1979). Furthermore, a particle initially moving on a circular orbit acquires a radial velocity and thereafter moves on a Keplerian ellipse. In a frame co-rotating with the perturbing satellite, all particles initially moving in circular orbits must follow similar paths after encounters. Thus, each perturbing satellite generates a standing wave. In the inertial frame, each particle moves on an independent Keplerian ellipse, but the pericentres of these elliptical orbits and the phases of the particles create a sinusoidal wave that moves through the ring with the angular velocity of the perturbing satellite. For a more complete discussion, see Shu (1984). Numerous such *density waves* have been observed in the rings of Saturn (see below) and perhaps also in those of Uranus (Horn *et al* 1989). The damping of these waves by collisions can result in a net exchange of angular momentum between the satellite and the ring particles. This phenomenon is similar to the dynamical friction studied in stellar dynamics.

The discovery of ten small satellites inside the orbit of Miranda during the Voyager 2 Uranus encounter has given a remarkable opportunity to test the predictions for shepherding of the Uranus rings. Porco and Goldreich (1987) showed that Cordelia and Ophelia are the inner and outer shepherds for the ε ring, and that Cordelia is an outer shepherd for the γ ring. They have demonstrated that these satellites are capable of confining the ε ring if the mass and the thickness of the ring are low enough. The outer edges of the δ and the γ rings can also be confined by these satellites, but the drag due to the planet's extended neutral hydrogen exosphere would require larger shepherd moons and, thus, poses a severe problem for the shepherding of the α and β rings (see below and French *et al* (1991)).

4. Ring phenomena

4.1. Saturn's broad rings

Saturn with its rings remains one of the truly beautiful objects in the sky. It is still one of the most requested and observed targets for small telescopes at observatories and planetaria. The ringed planet is also a popular symbol for the wonders of space. The magnificent images from Voyager 1 and 2 ensure that this will continue to be true for some time, although the superior cameras on the Cassini spacecraft are rapidly approaching Saturn and may provide even more stunning views.

Some years ago, the broad structure of Saturn's rings was characterized by ground-based observers. Figure 2 is a tracing of ring brightness by Dollfus (1970). Almost every feature in this brightness profile has a clear basis in the optical-depth profile observed in the most recent studies; for comparison, figure 3 shows the vertical optical depth from the Voyager 2 photopolarimeter stellar (PPS) occultation (Esposito *et al* 1983b).

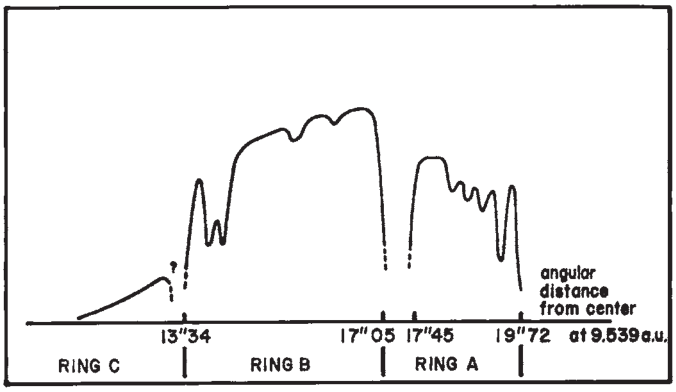

Figure 2. The overall structure of Saturn's rings as determined by ground-based observations. After Dollfus (1970).

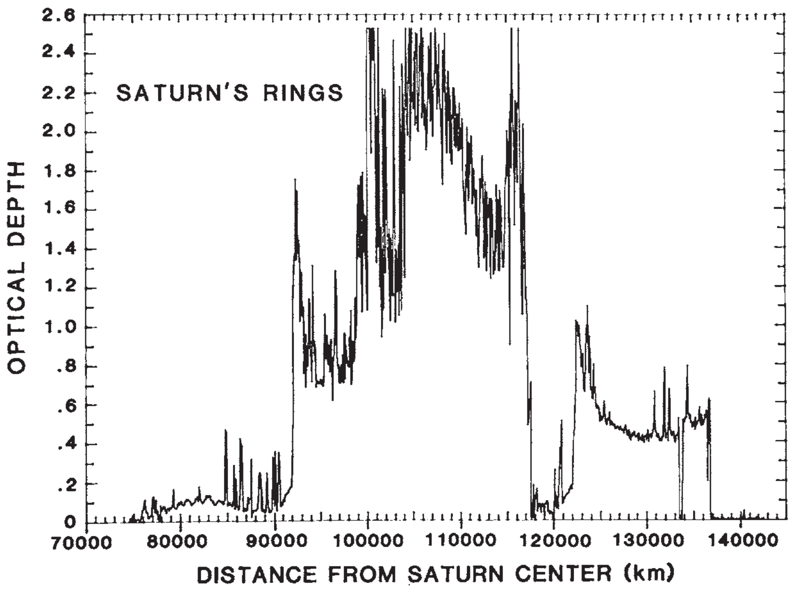

Figure 3. Optical depth of Saturn's rings measured by the Voyager PPS occultation. The resolution has been degraded by averaging the original data in bins of 600 measurements. Figure from Esposito *et al* 1983a The structure of Saturn's rings *Icarus* **56** 439–52, © 1983 Elsevier Science (USA), reproduced by permission of the publisher.

One notable aspect from figure 3 is the similarity of the inner edges of Saturn's B and A rings (at about 91 000 and 121 000 km). These similar features have not been explained by any known resonance with Saturn's moons. One explanation is that the gradual ramps are formed from a balance between collisions among the ring particles and the production of debris from meteoroid collisions. The movement of ring material by impacts from meteoroids is termed *ballistic transport* (Durisen *et al* 1989, 1992, 1996). The fragments from a meteoroid collision have distinct orbits that reintersect the rings. At a later ring crossing, the fragments collide with ring particles, imparting energy, momentum, and mass at that location. This transport modifies

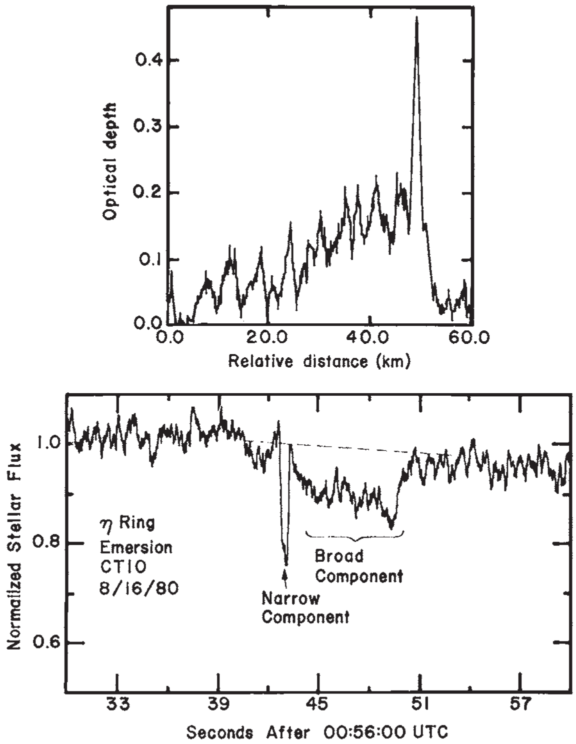

Figure 4. Top: Optical depth of Saturn's F ring from the Voyager PPS occultation. Reprinted with permission from Lane *et al* 1982 Photopolarimetry from Voyager 2 *Science* **215** 537, © 1982 American Association for the Advancement of Science. Bottom: Transmission of the Uranus η ring. Figure from Elliot *et al* 1981 Orbits of the nine Uranian rings *Astron. J.* **86** 444–55, © 1981 American Astronomical Society, reproduced by permission of the publisher.

the expected ring evolution due to slow spreading and resonant interactions, especially near the edges of opaque rings.

A number of features we see in Saturn's rings appear to have two components, one broad and one narrow. Figure 4 compares Saturn's F ring opacity to that of the Uranus delta ring. The Uranus delta ring also shows a similar structure (Elliot *et al* 1985). The phenomenon of narrow rings embedded in broader ones is thus more general than just Saturn's rings and may be related to multiple origins of the ring material, with the older ring particles more spread out.

We still do not have a good explanation for the abundant microstructure in Saturn's rings (see figure 5). The spacecraft data have demolished the earlier expectation that the rings were broad and homogeneous. Instead, we now know the rings are filled with numerous structures. Indications came first from the studies of the dark side of the rings and the ring-passage observations analysed by Lumme and Irvine (1979), and from the Pioneer 11 data (Esposito *et al* 1980). These studies did not have the resolution of Voyager, but they showed light leaking through that could not have come through a homogeneous ring. Still, it was quite unexpected when Voyager approached Saturn for the first time in 1980 (and even again, for the second time in 1981 with the higher resolution provided by the stellar occultation) that we would continue to discover more structure in the rings. The structure is apparent at all ranges. The shape of the power spectrum is approximately $1/f$ down to the noise level: i.e. we see structure at all scales in the rings, down to the best resolution we have ($\sim$100 m, Esposito *et al* (1983a)).

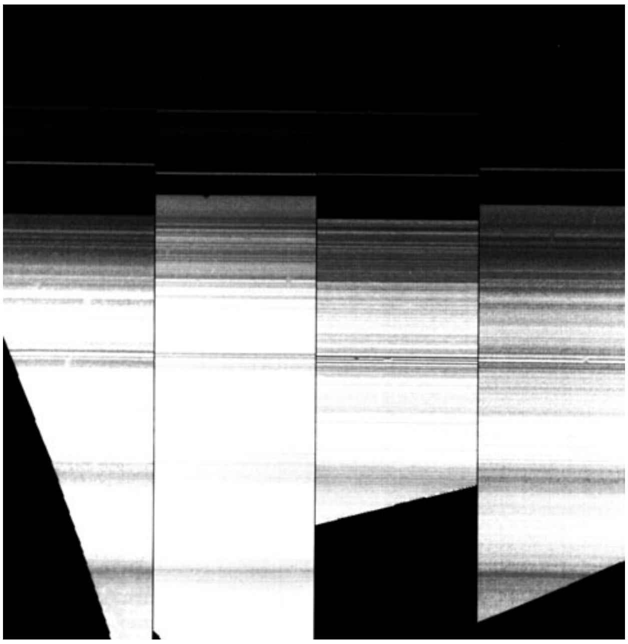

Figure 5. Small-scale structure in Saturn's B ring as seen by the Voyager camera at four different longitudes. Smallest features seen are about 20 km in width. NASA-JPL Voyager 2, 260–1473; see Smith *et al* (1982).

A proposed explanation for this structure is diffusional instability (see, e.g. Lin and Bodenheimer (1981), Ward (1981)); however, Wisdom and Tremaine (1988) have shown that this instability would not actually occur. Furthermore, Brophy and Esposito (1989) have shown that the optical-depth distribution is inconsistent with the model predictions. Recently, Schmidt *et al* (2001) suggested that this irregular structure may result from a 'viscous overstability' in the dense parts of Saturn's B ring. High-resolution studies from Cassini could confirm this explanation.

4.2. Waves

Much of the structure in Saturn's A ring is explained by resonances with Saturn's small moons, which excite density waves in the ring. These resonances are mostly of the form $m + 1 : m$, the ratio between the moon's orbital period and that of the ring particle. The ring phenomena produced are tightly wound spiral density waves similar to those that cause the spiral structure of galaxies (Shu 1984). The self-gravity of the rings provides a restoring force: this allows the wave to propagate away from the resonance, towards the perturbing moon. The Voyager PPS occultation and the radio occultation provided a very large set of waves to look at—approximately 50 density waves and a small number of bending waves (Esposito *et al* 1983a, b, Esposito 1986, Rosen 1989, Rosen *et al* 1991a, b). Figure 6 shows the Saturn Mimas 5 : 3 and Janus 2 : 1 density waves propagating outward in the rings. Why are these waves of interest? Simply, they provide a remote probe of the ring's nature. We cannot yet get our hands on the rings or even image an individual ring particle; thus, we are in the same situation as the plasma physicist in the laboratory: we cannot place our measuring instrument into the medium that we want to measure. These waves are diagnostics in the same way that waves sent through a plasma are plasma diagnostics—we analyse the dynamic response of the medium to these

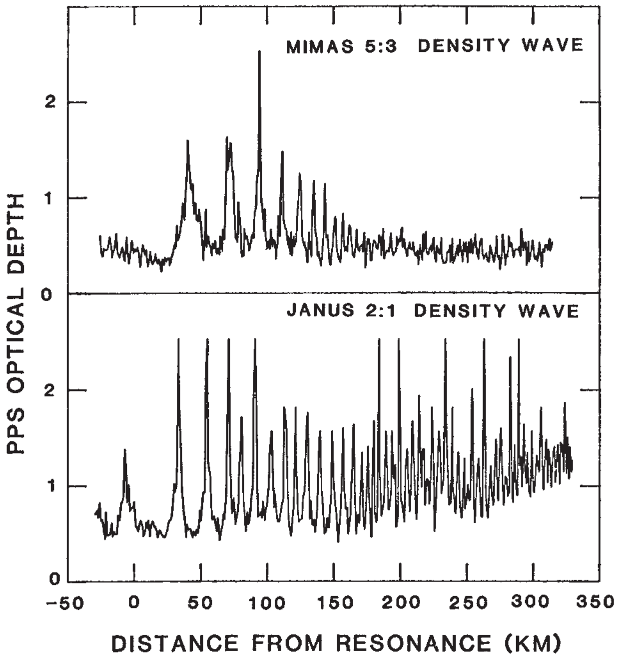

Figure 6. Two density waves in Saturn's rings. Note that the amplitudes are not small compared to the background optical depth and there is little resemblance to a pure sine wave. From Esposito *et al* (1983b).

waves and we are able to infer a number of physical properties: mass density, viscosity, vertical thickness. As an example, the total mass of Saturn's rings can be estimated to be about the same as its small moon, Mimas (Esposito *et al* 1983a).

The ability of the theory to reproduce the exact wave structure is more mixed. For the Mimas 5 : 3 density wave (figure 6), the general shape matches theoretical models (for example, Longaretti and Borderies (1986)). On the other hand, for the Janus 2 : 1 wave in figure 6 (the longest wave train and also the first wave seen in the Voyager photopolarimeter data), we are still a long way from a complete explanation. Part of the wave behaviour is understood. For example, the theoretical prediction for the wave crests' location is well matched by the waves that we see. The wave train includes 79 observed waves that are located as predicted by the linear theory (Shu 1984). From this wavelength behaviour, we estimate the ring mass density at the wave location to be about 70 g cm^{-2} (Holberg *et al* 1982, Lane *et al* 1982, Esposito *et al* 1983a). The derived mass density of the rings does not seem to be changed very seriously by more detailed analyses, which include nonlinear effects (see Shu *et al* (1985a, b)). However, these same models fail to predict the amplitudes of the wave crests, which remains an unsolved problem. Analysis of the 28 Sgr occultation gives a larger value for the ring mass by integrating over the derived size distribution (French and Nicholson 2000, Nicholson *et al* 2000). The best explanation of this discrepancy is that the 'particles' seen in the star occultation are actually underdense, perhaps temporary piles of rubble.

4.3. Spokes

Thirty-seven days before its closest approach to Saturn, Voyager 1 discovered dark, nearly radial, wedge-shaped markings (called *spokes*) in Saturn's B ring (Smith *et al* (1982);

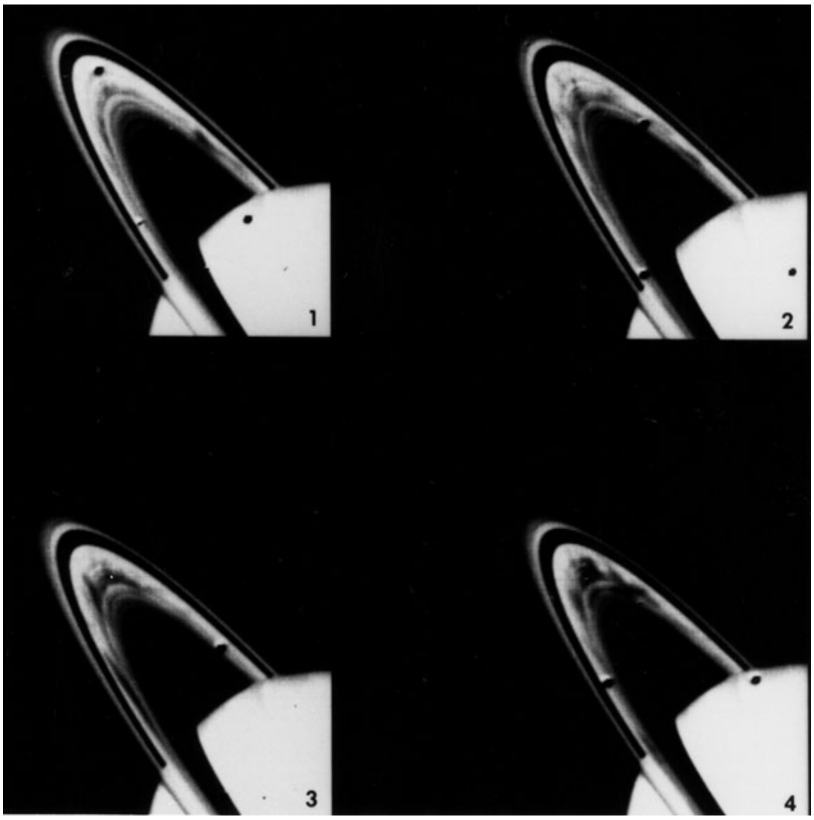

Figure 7. Voyager camera observations of spokes in Saturn's rings showing a range of spoke activity. Analysis shows that the strongest activity occurs at one particular magnetic longitude. NASA-JPL Voyager 2 photos.

see figures 7 and 8). It was quickly determined from Voyager high-phase-angle pictures that these spokes contain a large proportion of micron-sized particles.

The small size of the particles explains naturally why they appeared dark on Voyager's approach and bright after it: particles about the same size as the light wavelength will preferentially scatter light forward into the angles Voyager observed looking back towards the Sun. These small particles are also more easily moved by electric and magnetic forces, since their charge-to-mass ratio can be large. This consideration leads naturally to a possible connection with electromagnetic effects. The Voyager planetary radio astronomy experiment discovered both broadband electrostatic discharges (*Saturn electrostatic discharges*, or *SED*) and a strong source of kilometric wavelength radiation (*Saturn kilometric radiation*, or *SKR*). An interrelation between spokes, SED, and SKR seems plausible, since power spectral analysis of spoke activity (Porco 1983) found a significant peak with period 640.6 ± 3.5 min, consistent with the 639.4 min period of rotation in Saturn's magnetic field. Thus, the spokes are preferentially created at a peculiar longitude of Saturn that is also known to emit SKR. The most plausible explanation for this correlation would be the existence of a magnetic anomaly in Saturn's dipole field creating the anomalous behaviour of the magnetosphere near the rings.

One of the most puzzling aspects of spokes is that they extend across the B ring for many thousands of kilometres. Spoke particles do not actually move radially but are observed close to their points of initial elevation. Smith *et al* (1982) observed a narrow radial spoke grow to a

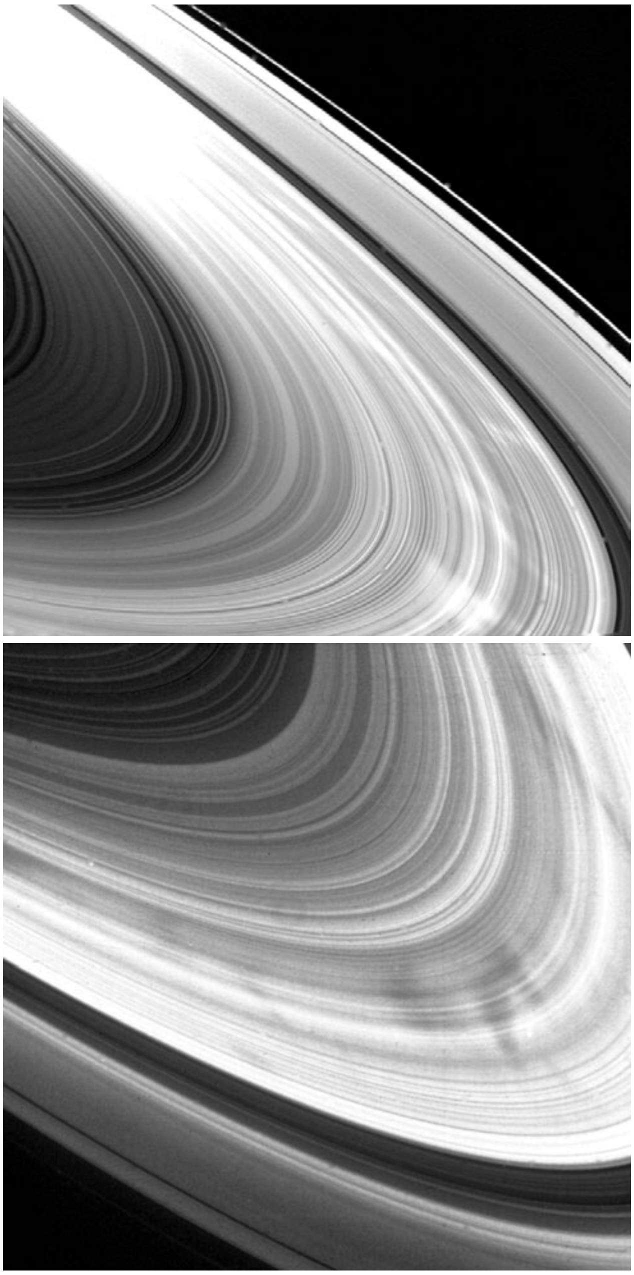

Figure 8. Spokes seen in forward scattered light (i.e. backlit by the Sun) are now brighter than the surrounding ring: this and similar Voyager images indicate that the spoke particles have a size near the wavelength of visible light. Top: NASA-JPL Voyager 1, PIA02269. Bottom: NASA-JPL Voyager 2, PIA02275.

length of 6000 km in $<$5 min. If the spokes are the manifestation of a discharge that proceeds along the length of a spoke, then this formation time implies a minimum disturbance speed of 2×10^6 cm s^{-1}. This is much greater than any expected mechanical propagation speed for the rings; for example, velocity dispersion of the larger ring particles is $\lesssim$0.5 cm s^{-1}.

Voyager measurements have shed some light on this. By measuring the motions of two narrow, forming spokes (including the one reported in Smith *et al* (1982)), Grün *et al* (1984) determined that inside the co-rotation point, the trailing edges travel with the angular speed of the magnetic field, thereby remaining radial, while the leading edges move at Keplerian speeds. After formation, both edges tilt away from radial at the Keplerian rate. (Both edges of all other spokes measured in that study moved with Keplerian motion.) The angle of the wedge produced by the differential motion between edges is taken to be a measure of the time during which the spoke was active. Typical active times inferred from wedge-angle measurements of old spokes were 1–3 h. Thus, spokes form in minutes and persist for hours. A possible cause is the impact of meteoroids on the rings, which creates a small puff of ionized gas (Morfill *et al* 1983a, b). One possibility recently proposed is that they are the manifestation of magnetosonic waves in the partly ionized ring disk. This could explain their rapid propagation following the impact of a meteoroid (Tagger *et al* 1991). Cuzzi and Durisen (1990) propose that the spokes are more likely to occur near dawn (as observed) because meteoroid impacts are more energetic on the night side of the planet where the ring particle orbital velocity adds to Saturn's orbital velocity.

4.4. Narrow and eccentric rings

Until the discovery of the Uranus rings in 1977 (Elliot *et al* 1977), it seemed natural that all rings should be circular. Mutual collisions would cause eccentric motions to damp out and circularize the particle orbits. The rings of Uranus (figure 9) instead turned out to be eccentric, inclined, narrow, and sharp edged! Most of these oddities can now be explained as due to the effects of nearby satellites (Goldreich and Tremaine 1982, Borderies *et al* 1984, Dermott 1984). To avoid the smearing out of an elliptical ring, Goldreich and Tremaine (1979) invoked the self-gravity of the ring particles themselves to create a precession of the ring that just counteracts the precession caused by the planet's gravity. This makes a very explicit prediction for the mass density of the rings of Uranus that is, however, not confirmed by the spacecraft observations (Goldreich and Porco 1987, Esposito and Colwell 1989, Esposito *et al* 1991, French *et al* 1991). It is likely that particle collisions can play a critical role. A possible mechanism involving collisions is discussed by Chiang and Goldreich (2001).

The Uranus rings have provided a prototype for understanding other narrow, eccentric features in Saturn's rings (for example, Porco *et al* (1984a, b); Porco and Nicholson (1987), Porco (1990)). Likewise, we expect that close study of the Saturn features by Cassini may give some insights that will help explain some of the puzzles of the eccentric Uranus and Neptune rings.

4.5. Dusty rings

Dust is found in all the planetary ring systems (Burns *et al* 1984, Ockert *et al* 1987, Smith *et al* 1989, Esposito *et al* 1991, Showalter *et al* 1991, Burns *et al* 2001), generally in faint bands most easily visible when backlit by the sun (indicating that we are seeing particles of about 1 μm or less in radius). The majority of the dust is concentrated near the equator. The dust in these rings is likely derived from nearby satellites (Burns *et al* 1980, Colwell and Esposito 1990a, b, Burns *et al* 1999), and dust may also coat the moons' surfaces. The dust dynamics are determined by the planet's gravity and magnetic field, solar radiation pressure, local plasma, and gas density (Horanyi 1998). If small enough dust particles become charged, they co-rotate with the planetary magnetic field. Radiation from the sun can charge the dust grains and cause a relativistic drag force (Mignard 1984). Furthermore, the dust is ground down by a continual flux of micrometeoroids (Burns *et al* 1980) and lost.

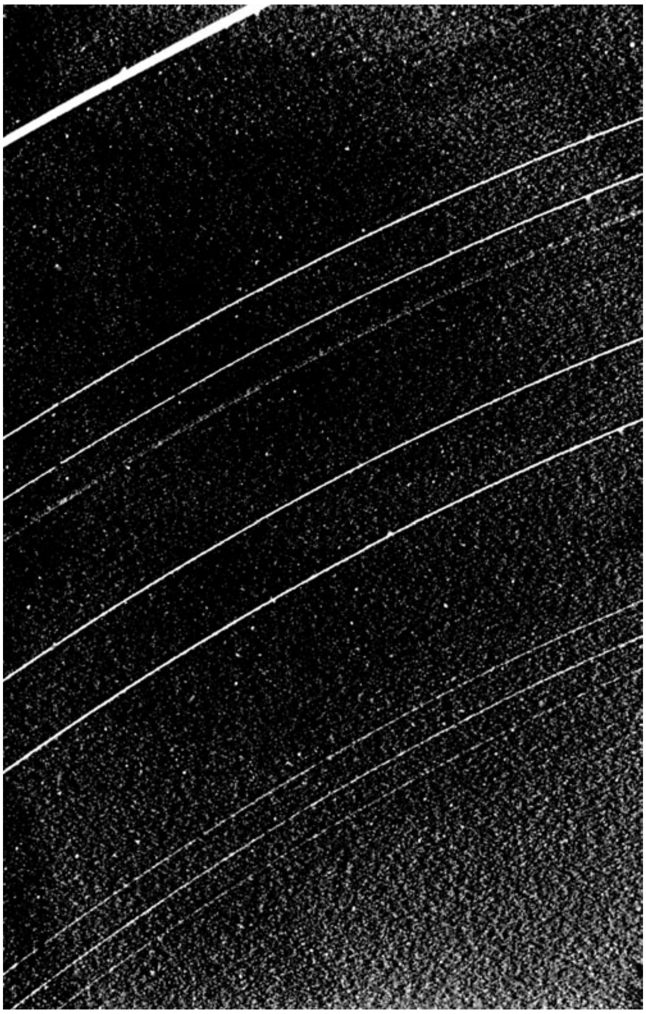

Figure 9. Uranian rings are seen in an image obtained by Voyager 2 from a distance of about a million kilometres as the spacecraft approached Uranus. The threadlike rings, which are for the most part densely packed with particles, are only a few kilometres wide. They are separated by hundreds of kilometres of virtually empty space. A new ring originally designated 1986U1R (now known as the λ ring) is barely visible between the outermost ring (ε) and the next bright ring (δ). The rings reflect only 1% of the incident light. NASA-JPL Voyager 2, PIA019.77.

The premier 'dusty' ring surrounds Jupiter (figure 10), whose light is dominated by scattering from small particles. The dust is derived from small satellites (Ockert-Bell *et al* 1999), has its orbits modified by orbital evolution due to plasma drag, and spreads vertically and horizontally. Just as the gravity of moons sculpts the broader rings of macroscopic particles, resonances with Jupiter's magnetic field may cause boundaries and other features in the ring (Schaffer and Burns 1987) and perturb the particles into inclined orbits, which explains the observed vertical thickness of the ring halo (Schaffer 1989).

Galileo observations (figures 11 and 12) have refined our picture of Jupiter's rings, showing clearly its three components: (1) a radially confined and vertically extended halo that rises abruptly; (2) a 6500 km wide flattened and patchy main ring whose outer edge is bounded

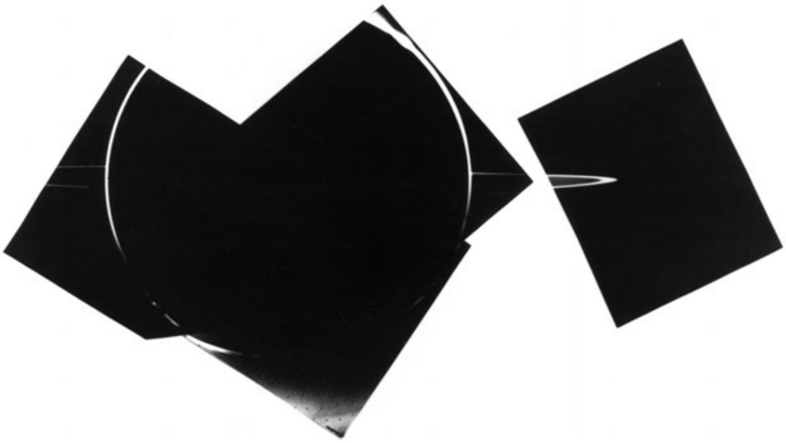

Figure 10. One of the most spectacular of the Voyager 2 images obtained from inside the shadow of Jupiter. Looking back toward the planet and the rings with its wide-angle camera, Voyager took these photos on 10 July 1979 from a distance of 1.5 million kilometres. The ribbonlike nature of the rings is clearly shown. The planet is outlined by sunlight scattered from a haze layer high in the atmosphere. On each side, the arms of the ring curving back towards the spacecraft are cut off by the planet's shadow as they approach the brightly outlined disk. NASA-JPL Voyager 2 photo mosaic.

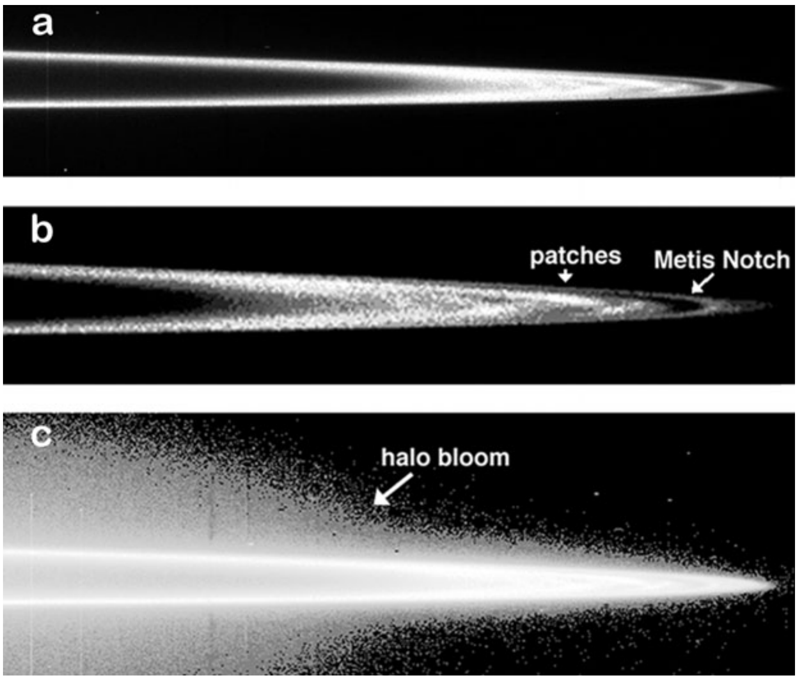

Figure 11. A Galileo view of the Jovian ring's west ansa, processed in three different ways to highlight several features: (*a*) a stretch to contrast the main ring's diffuse inner boundary with its much sharper outer boundary; (*b*) a stretch that emphasizes the patchy main ring, including a brightness decrease at the location of the Metis orbit, the *Metis notch*; and (*c*) a stretch to reveal the faint cloud of material above and below the main ring and the location where the vertical extent of the ring system rapidly increases inwards, as the halo 'blooms.' (*a*) NASA-JPL Galileo, PIA00538. (*b*) and (*c*) NASA-JPL Galileo PIA01622; see Ockert-Bell *et al* (1999).

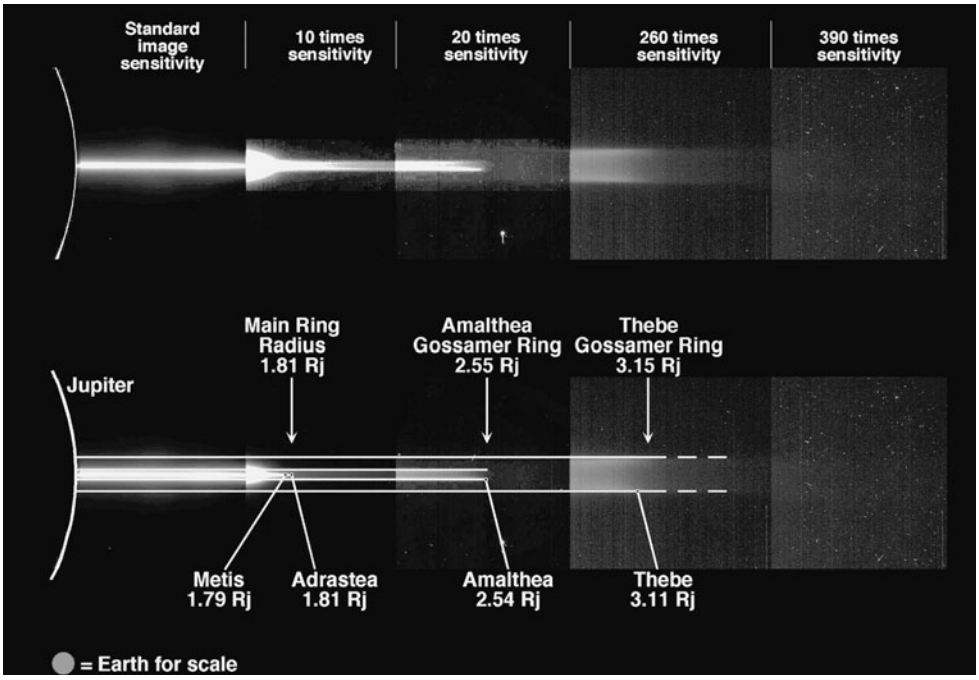

Figure 12. The Galileo mosaic C10, stretched to clarify individual elements of Jupiter's ring. The bottom frame is unstretched. The top frame shows clearly the faint halo, the gossamer rings, and their crudely rectangular end profiles. NASA-JPL Galileo, PIA01623; see Ockert-Bell *et al* (1999).

by the orbit of Adrastea; and (3) a pair of exterior gossamer rings derived from the satellites Amalthea and Thebe, whose orbits circumscribe these rings (Burns *et al* 1999, 2001). These moons, which are thus parents of the visible dust (Burns *et al* 1980), are sometimes referred to as *mooms*, a contraction of 'moon' and 'mom.'

The phase curves of Jupiter's main ring (see figure 13) are compatible with a power-law size distribution with index $q = 2.5 \pm 0.5$ (Showalter *et al* 1987, Brooks and Esposito 2000). Galileo NIMS spectra at longer wavelengths (McMuldroch *et al* 1999, Brooks *et al* 2001) show that this power law steepens at sizes $r \geqslant 10\ \mu$m, perhaps indicating erosion of the particle size distribution by drag effects (Throop *et al* 2002).

Dust is also prominent in Saturn's E, F, and G rings (Smith *et al* 1982), in Neptune's rings (Smith *et al* 1989), and between the rings of Uranus, as evident from the backlit view of figure 14. However, dust is mostly absent from Saturn's main rings except in the localized spokes. Saturn's E ring is probably dominated by 1 μm grains derived from Enceladus (Baum *et al* 1980, Showalter *et al* 1991, Hamilton and Burns 1994).

4.6. Clumpy rings

Prior to the spacecraft observations of the past twenty years, it was possible to hold an idealized model of rings, which among other attributes assumed that rings possess azimuthal symmetry. Some azimuthal variations were known in Saturn's A ring (Camichel 1958, Lumme *et al* 1977), but the actual extent of longitudinal heterogeneity was mostly unexpected. We have now observed plentiful examples. Among this group, which includes Saturn's F ring and the Uranus η ring, two cases are prominent: Saturn's Encke Gap ringlet (figure 15) and Neptune's

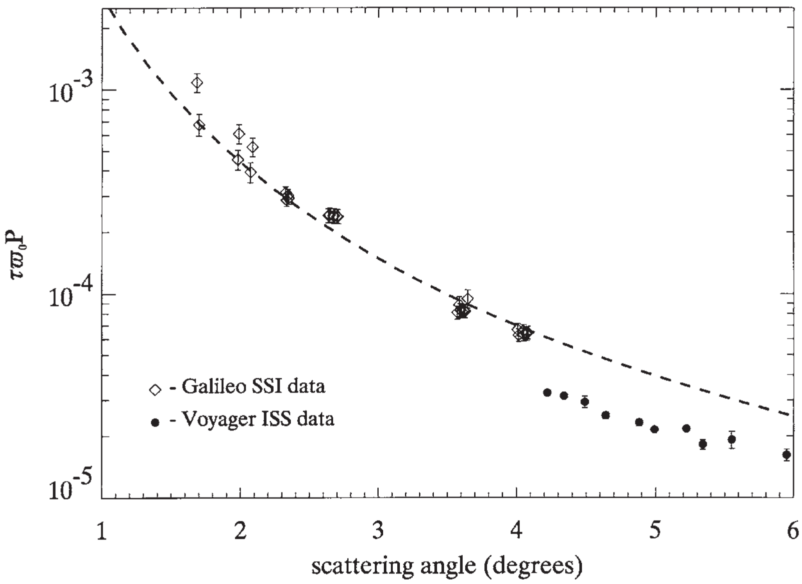

Figure 13. Jupiter's main ring phase curve. The ring brightness is plotted against the angle between the illumination direction and the viewing direction. (*scattering angle*: this is 180° minus the phase angle). The offset between the Voyager and Galileo data may be due to errors in the calibration of their relative sensitivity. The Galileo images extend the Voyager data to smaller scattering angles and show a similar power-law size distribution for the Jupiter main ring particles. For reference, a theoretical phase curve for particle size distribution with $q = 2$ is fitted through the Galileo camera observations. After Brooks *et al* (2002).

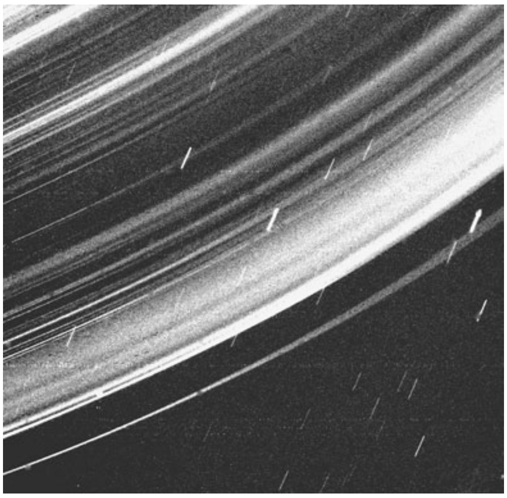

Figure 14. A backlit view of the Uranus rings shows numerous rings previously unseen from Earth or by Voyager on its approach. This brightening is similar to that seen for Saturn's spokes (figure 8) and Jupiter's ring (figure 10), showing that these new rings are mostly composed of micron-sized dust. The classical nine rings of Uranus can be found among the rings shown in this photograph but they are undistinguished. Only the newly discovered λ ring (see figure 9) is especially bright. NASA-JPL Voyager 2, PIA001.42, FDS 26852.19.

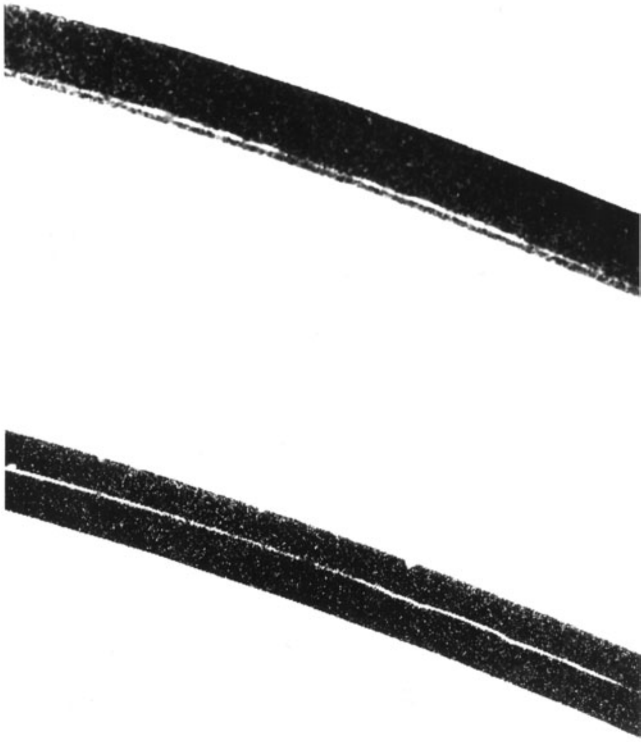

Figure 15. Within the Keeler gap in Saturn's A ring lie at least two discontinuous ringlets. This Voyager 2 picture, with a resolution of about 10 km, shows one of these rings to be kinky. The kinks are spaced about 700 km apart, approximately ten times more closely than the F ring kinks photographed by Voyager 1. NASA-JPL Voyager 2, PIA01381.

Adams ring (figure 16). The irregular, kinky structure of the Encke Gap ringlet was attributed to small nearby moons; and, in fact, this moon was found there in a re-analysis of the Voyager camera images (Showalter 1991). The Neptune ring structure includes a set of five small arcs in a longitudinal range of only 25° (Porco 1991). The Voyager pictures show a very dim but continuous complete ring underlying these arcs, which was unfortunately too transparent to be detected from Earth-based occultations (Nicholson *et al* 1990). A model of Goldreich *et al* (1986) explained the arcs through particles caught in co-rotation resonances with large, nearby inclined moons. The Voyager pictures did not show any moons as large as predicted, but the radial excursions of the ring particles clearly show the influence of Neptune's moon Galatea, and the particles' azimuthal distribution can be consistent with Goldreich's model (Porco 1991). Unfortunately, collisions between the ring particles are likely to eject them from the weakly confining resonances, and we must consider this model incomplete. A possible improvement is that additional unseen moons can assist in this confinement (Sicardy and Lissauer 1992), similar to the moon Pan's effect on the Encke ringlet.

The azimuthal structure in Saturn's narrow, slightly elliptical F ring (often referred to as *braids*, figure 17) can also be attributed to unseen moons (Kolvoord *et al* 1990, Kolvoord and Burns 1992). In the model of ring creation by the destruction of a moon, these hypothesized nearby moons may be the largest fragments of a satellite that was shattered to form the ring (see below).

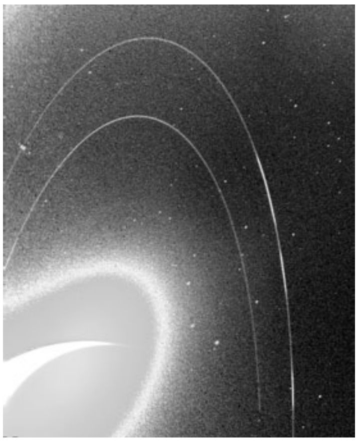

Figure 16. This Voyager 2 image shows the Neptune ring system in forward scattering geometry (phase angle of 134°). Clearly seen are the three ring arcs and the Adams and Leverrier rings. The direction of motion is clockwise; the longest arc is trailing. The resolution in this image is about 160 km. NASA-JPL Voyager 2, PIA02207.

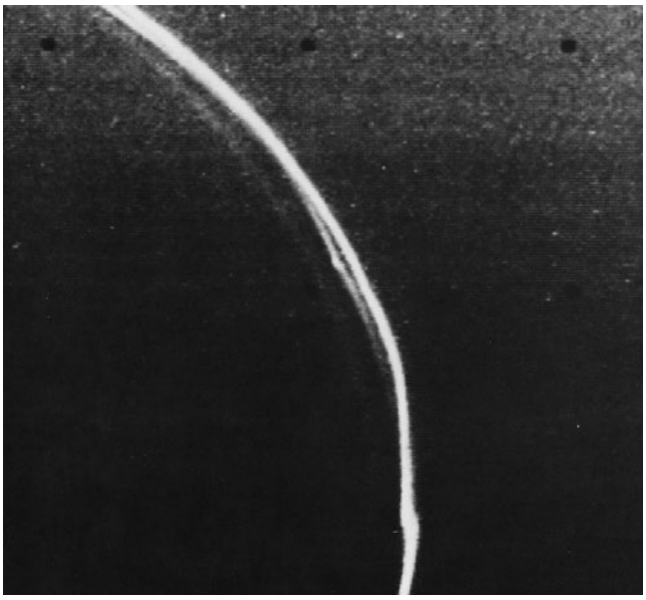

Figure 17. One of the most exciting photos of the Voyager 1 Saturn encounter shows the F ring from a distance of 750 000 km. At a resolution of about 15 km, this outer ring suddenly revealed a complex braided structure. Two narrow bright rings that appear braided are visible, in addition to a broad diffuse component apparently separated from them by about 100 km. Also visible is a kink, or knot, where the ring seems to depart dramatically from a smooth arc. NASA-JPL Voyager 1, FDS 34930.48, PIA02283.

The F ring was discovered by the author as part of the Pioneer 11 imaging photopolarimeter team (Gehrels *et al* 1980). The clumpy nature of the ring was confirmed by Voyager (Smith *et al* 1981, 1982). Although it originally appeared to be a clear example of a shepherded ring (see section 3.2) since it lies between two nearby moons, Pandora and Prometheus, current opinion is not so clear. The torques from these moons on the ring do not actually balance (Showalter and Burns 1982)! Further, the orbits of the shepherds are changing (Nicholson *et al* 1996, French *et al* 1999). One suggestion is that their orbits are responding to as-yet-unseen moonlets within the F-ring region, which may also be the source of the ring material (Cuzzi and Burns 1988, Murray *et al* 1997, Barbara and Esposito 2002).

Clumps in the F ring appear abruptly, perhaps produced by impacts of interplanetary meteoroids into unseen parent bodies (Showalter 1998) or from material knocked off by collisions of the parent bodies themselves (Barbara and Esposito 2002). Observations of Saturn's edge-on rings using the Hubble Space Telescope in 1995 led to reports of previously undetected moons outside the A ring. Unfortunately, no consistent orbits were found and further, such moons should have been seen by Voyager. Most likely, they were just more of those temporary clumps as seen by Voyager (Poulet *et al* 2000, Barbara and Esposito 2002). This conclusion provides good support for the model of Cuzzi and Burns (1988), where a belt of smaller (0.1–10 km) moonlets fills a 2000 km band surrounding the F ring. Analysis by Bosh *et al* (2002; see figure 18) shows that the colour of the F ring is compatible with the power-law size distribution with index $q \sim 2$. This value is similar to those from Jupiter's main ring (Brooks *et al* 2002) and Saturn's G ring (Throop and Esposito 1998). French and Nicholson (2000) found that power-law size distributions fit the Saturn occultation data in the range $2.7 < q < 3.1$; see table 2.

Saturn's tenuous G ring, which is about 7000 km wide and centred on orbital radius 168 000 km, may also be derived from unseen parent bodies. Its light at all angles is dominated by dust, however. Throop and Esposito (1998) favour a power-law size distribution with $1.5 < q < 3.5$. Both Canup and Esposito (1997) and Throop and Esposito (1998) demonstrate that this size distribution would be a natural result of disruption of a progenitor parent satellite.

Saturn's E ring extends over hundreds of thousands of kilometres in radius, with its brightness peaked near the orbit of Enceladus. Its major source is likely from external impacts

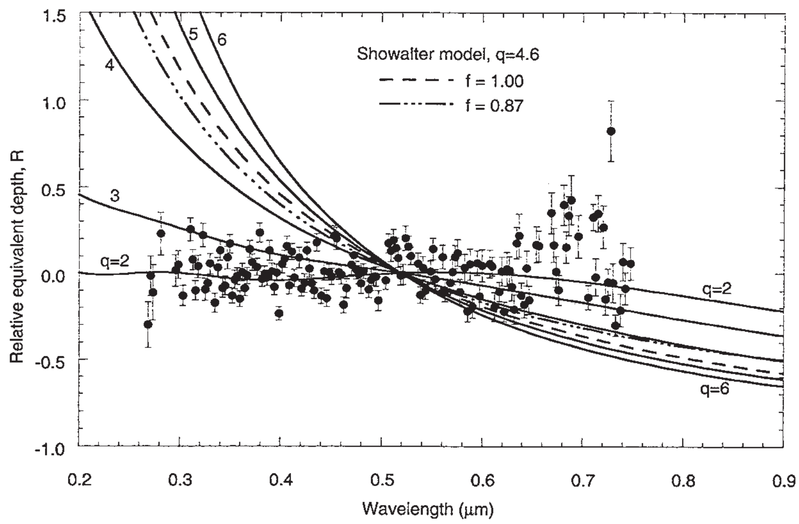

Figure 18. Relative total brightness of Saturn's F ring from Hubble Space Telescope data during the ring plane crossing of 1995. Models of Showalter *et al* (1992) for dust fractions $f = 1.00$ and $f = 0.87$ are shown. Much better fits to the data are given by power-law size distributions with indices $q = 2$ or $q = 3$. Figure from Bosh *et al* 2002 Saturn's F ring *Icarus* at press © Elsevier (USA), reproduced by permission of the publisher.

Table 2. Regional particle size distributions.

Ring region	Radius range (km)	q[a]	$a_{\min}$[b] (cm)	$a_{\max}$[b] (m)	a_{eff}[c] (m)	a_{eff}[c,d] (m)	σ/τ_g[e] (gm cm^{-2})
C	74 490–91 983	3.1	1	10	2.3	$\leqslant$1.2–2.8	149
B	91 983–117 516	2.75	30	20	8.3	5.7–8.8	816
Cassini Division[f]	117 516–122 053	2.75	0.1	20	7.0	$\leqslant$1.1–4.5	582
A (inner)	122 053–133 423	2.75	30	20	8.3	11.2–12.2	816
A (outer)	133 745–136 774	2.9	1	20	6.0	9–10.7	455

[a] q—power-law size index.
[b] $a_{\min}$, $a_{\max}$—smallest and largest particle in size distribution.
[c] a_{eff}—cross-section averaged mean particle size.
[d] Showalter and Nicholson (1990).
[e] σ/τ_g—the ring surface mass density per unit geometrical depth, proportional to the particle density, assumed here to be $\rho = 1$ gm cm^{-3}.
[f] The Cassini Division particle size distribution is not well determined from these observations.
Table from French R G and Nicholson P D 2000 Saturn's rings II. Particle sizes inferred from stellar occultation data *Icarus* **145** 502–23, © 2000 Elsevier Science (USA), reproduced by permission of the publisher.

on that moon; it may in some way be self-sustaining (Hamilton and Burns 1994). The ring's colour is not compatible with a simple power law. The most recent models for the E ring are by Juhasz and Horanyi (2002).

4.7. Summary

The structures and phenomena seen in planetary rings show a rich variety of physical processes, particularly in the interactions between small moons and nearby rings.

5. Age and evolution of rings

5.1. Introduction

As described by Harris (1984), the rings of the planets likely result from the same process that created the regular satellites. Like the ring particles, the satellite orbits are prograde, equatorial, and nearly circular. A question that immediately arises is whether rings are (1) the uncoagulated remnants of satellites that failed to form, or (2) the result of a disruption of a pre-existing object. A related question highlighted by the apparent youth of the rings is whether this latter process of ring creation by satellite destruction continues to the present time. This possibility thus mixes the origin of the rings with their subsequent evolution. Whatever their origin, the sculpted nature of the rings of Saturn, Uranus, and Neptune requires active processes to maintain them (see section 4).

Because of the short timescale for viscous spreading, gas drag, particle coagulation, and transport of momentum to the forming planet, Harris (1984) argues that rings did not form contemporaneously with their primary planets but were created later by disruption of satellites whose large size had made them less subject to the early destructive processes. The pieces of the disrupted satellite are within the Roche zone, where tidal forces keep them from coagulating. This explains naturally the presence of shepherd satellites and ringmoons around the various giant planets as the largest pieces remaining after the destruction.

Conversely, both Lissauer *et al* (1988) and Ip (1988) have shown that it is very unlikely for a moon large enough to create the Saturn rings to be disrupted by the meteoroid flux recorded on the surfaces of the remaining Saturn satellites. Dones (1991) argues that a comet may have come too close to Saturn and been disrupted to form the rings. Harris (1984) notes that the ring disruption hypothesis is particularly attractive for the Uranus rings; below, arguments are presented that processes currently active in the Uranus and Neptune systems may require some very recent ring origins.

5.2. *Age of the rings*

Estimates of the age of the rings can discriminate between possible scenarios for ring formation. If lifetimes of some components are much less than the age of the solar system, those parts cannot have a primordial origin. This argument indicates the recent origin of the material we observe in the Jovian ring (Burns *et al* 1980, 1999), Saturn's A ring (Esposito 1986), Saturn's F ring (Cuzzi and Burns 1988), the Uranus rings (Esposito and Colwell 1989, Colwell and Esposito 1990a), and the Neptune rings (Smith *et al* 1989, Colwell and Esposito 1990b, 1992, 1993). Micrometeoroid bombardment of Saturn's rings is 'interplanetary pollution,' which should darken them rapidly (Cuzzi 1998).

The narrowness of the observed rings of Uranus and Neptune raised the first concern about the age of these rings. Because the interparticle collision time is short, less than half the orbital period for optically thick rings (Stewart *et al* 1984), the particles collide and interchange momentum, causing the ring to spread (see section 3). Modelling a narrow ring as a fluid of single-size particles, one can define a local kinematic viscosity:

$$\nu \approx \frac{c^2}{2\Omega}\left(\frac{\tau}{1+\tau^2}\right), \tag{3}$$

where c is the interparticle random velocity, Ω the mean motion, and τ the optical depth (Cook and Franklin 1964). Even if the collisional velocity is minimized, the ring particles have a finite size, so that just the Kepler shear across a particle diameter will provide a nonlocal contribution to the viscosity for dense rings. For a more complete discussion, see Salo *et al* (2001). The minimum viscosity would be achieved if random motions vanish, in which case the ring behaves as an incompressible fluid (Borderies *et al* 1985). This gives

$$\nu_{\min} = \Omega\left(\frac{\sigma}{\rho}\right)^2, \tag{4}$$

where σ is the surface mass density of the ring and ρ the density of the ring particle. Modelling the ring spreading as a diffusion process leads immediately to the lifetime of a narrow ring of width Δr. The lifetime is

$$\Delta t \approx \frac{\Delta r^2}{\nu}. \tag{5}$$

For the Uranus rings we find $\sigma_{\min} = 80\,\mathrm{g\,cm^{-2}}$ (Gresh *et al* 1989) for $\rho = 1.4\,\mathrm{g\,cm^{-3}}$ (average for the Uranus satellites, Tyler *et al* (1986)), and $\Delta r = 100\,\mathrm{km}$ (maximum width of the ε ring) yielding $\nu_{\min} > 1\,\mathrm{cm^2\,s^{-1}}$ and thus, $\Delta t \lesssim 10^6$ years. Clearly, these rings must be confined, most likely by shepherding satellites (Goldreich and Tremaine (1980), section 3).

A major success of the Voyager encounter was the discovery of the satellites shepherding the ε ring (Smith *et al* (1986), Porco and Goldreich (1987), see figure 9). However, the apparent lack of other satellites to shepherd the other Uranus rings is also significant. This may be because the other shepherds were too small to be seen by the Voyager cameras ($R < 10\,\mathrm{km}$, Smith *et al* (1986)). The shepherds (seen and unseen) could then confine all the rings, preventing the very short lifetimes associated with unconstrained spreading.

5.3. Age of the Jupiter rings

The brightness of Jupiter's rings in forward-scattered light shows that many of the particles are about the same size as the wavelength of visible light. Such small particles can only persist for 10^3 years or less before being destroyed by sputtering or being dragged into the planet by interactions with the local plasma. The best way to resupply these rings is by meteoroid bombardment of small moons of Jupiter (Burns *et al* 1999) that eject dust into orbit around the planet.

5.4. Age of the Saturn rings

Spreading of Saturn's A ring due to mutual collisions among the particles (Esposito 1986) and darkening of the rings due to meteoroid material that coats their surfaces (Cuzzi 1995) both give ages much shorter than the solar system. It is hard to reconcile such youthful aspects with the large mass of Saturn's rings (perhaps equal to that of the moon Mimas). If Saturn's rings were created by the destruction of one of Saturn's moons (see below), this would be a very rare event in solar system history and thus unlikely to have occurred in just the last billion years or less. An alternate explanation of the destruction of a close-passing comet (Dones 1991) is also a very rare and unlikely event.

5.5. Age of the Uranus rings

A strong argument for the youth of rings is related to the rates of momentum transfer between the objects in the Uranus ring system (Esposito and Colwell 1989). These rates were first considered in light of the Voyager data by Goldreich and Porco (1987). As discussed above, angular momentum flows outward through an unperturbed disk carrying the viscous torque (for particles in Keplerian orbits):

$$T_{\mathrm{v}} = 3\pi\sigma\nu\Omega r^2. \tag{6}$$

We believe that the narrow rings of Uranus do not spread because an inner shepherd supplies this torque at the inner boundary, while an external shepherd carries it off at its outer edge. For the Uranus ε ring, we know the sizes and locations of the two shepherds and can estimate their masses from their size (Porco and Goldreich 1987). Lower limits to the mass of the ε ring can be inferred from the radio occultation results (Gresh *et al* 1989, Gresh 1990). For $\sigma > \sigma_{\min} = 80\,\mathrm{g\,cm^{-2}}$, the mass of the ε ring $M_{\mathrm{e}} > 10^{19}$ g. Since this is only a lower limit, it leaves open the possibility that the ε ring is more massive than the shepherds! If the ring is more massive than the shepherds, transferring momentum to them cannot significantly slow the spreading. However, the mass of the inner shepherd Cordelia is some three times the minimum mass of the ε ring (with an uncertainty of perhaps a factor of 2, Porco and Goldreich (1987)); so as long as M_{e} is close to its minimum value, this difficulty is avoided. Goldreich and Porco (1987) show that, in this case, the satellites are massive enough to supply and carry off the viscous torque T_{v}.

However, a lower limit to the viscous torque may be established by considering the drag on ring particles from the extended Uranus exosphere. The viscous torque must exceed the drag torque, or otherwise the outer edge would be dragged inwards by the transfer of momentum as the ring particles plough into the exosphere. The excess torque, $T_{\mathrm{excess}} = T_{\mathrm{v}} - T_{\mathrm{D}}$, is carried off by the resonance coupling to Ophelia. This momentum transfer causes Ophelia to evolve outwards away from the ring, and the ring spreads, maintaining its sharp outer edge at the slowly changing location of the Ophelia resonance.

The minimum viscous torque is thus $T_{\mathrm{v}} = T_{\mathrm{D}}$. At the ε inner edge, a resonance transfers the momentum of the inwardly diffusing ring particles to Cordelia. This momentum transfer,

$T_v + T_D > 2T_D$, causes Cordelia's semimajor axis to decrease. Since the mass of Cordelia is known, we can estimate how long it would require for Cordelia to have evolved inwards to its current separation, assuming the minimum torque and zero initial separation. The maximum duration of this shepherding is thus $t_{max} = \Delta L/2T_D$, where ΔL is the total change in angular momentum, and T_D is 9×10^{16} ergs (Goldreich and Porco 1987). This calculation gives $t_{max} = 6 \times 10^8$ years, considerably smaller than the age of the solar system (Esposito and Colwell 1989)! Cordelia could not have transferred this momentum to a larger inner moon, since none exists. Further, it could not have transferred it to one of the larger outer moons through a resonance that may have existed in the past, since capture into a resonance with an outer moon is not possible (Peale 1986), given the tidal expansion of the orbit of the larger outer satellite and the shrinking of Cordelia's orbit. This age, t_{max}, provides a strong upper limit because only minimum values for the torque, T_v, have been considered. In the minimum case where $T_v = T_D$, no torque is transferred to Ophelia while a torque $T_v + T_D = 2T_D$ is transferred to Cordelia, causing it to evolve inwards. Even shorter ages are implied for possible shepherds of the α and β rings.

One proposed solution to the short lifetimes of the Uranus rings is that dust, rings, and small moons are continually created by disruption of larger objects (Esposito 1986, Esposito and Colwell 1989, Colwell and Esposito 1990a). Esposito and Colwell propose two families of objects too small to be seen by Voyager. Small satellites $R \lesssim 10$ km are *ring precursors*. Belts of particles $R \sim 100$ m are called *moonlet belts*. These are similar to the material proposed to create Saturn's F ring by Cuzzi and Burns (1988; see also Barbara and Esposito (2002)). Evolutionary calculations that include both fragmentation and accretion yield bimodal size distributions consistent with this expectation. Meteoroid ejecta from rings, moons, and moonlet belts by gas drag lead to a continuous low-optical-depth sheet of dust in the main ring system, with the highest optical depth near the ε ring, where gas drag is slower. At the location of a moonlet belt, a dust band would be visible. Esposito and Colwell (1989) propose that these processes, along with variations in the widths, optical depths, and size distributions of the moonlet belts, account for the variety of forms of dust bands seen by Voyager at Uranus, thus giving an explanation for the structure seen in figure 14.

5.6. Age of the Neptune rings

The azimuthal variability of Neptune's rings is another strong indication of youth. Although Goldreich *et al* (1986) have shown how the arcs might be maintained, and Porco (1991) has shown that the Voyager observations are consistent with this model (see above), nonetheless, interparticle collisions will allow particles or their fragments to escape the resonance. Particles in orbits outside the small range of the co-rotation resonance will rapidly circulate to fill the entire ring circumference, creating a complete ring. Furthermore, recent Earth-based observations (Dumas *et al* 1999, Sicardy *et al* 1999) show that the exact ring location is outside the predicted location from Goldreich's model at the 42 : 43 Galatea resonance. Fortunately, a different resonance may be able to provide the confinement (Namouni and Porco 2002). Thus, the cause of the extreme azimuthal structure observed in Neptune's Adams ring is still not clear and quite unlikely to be a remnant of the formation of Neptune. It is more likely the result of recent catastrophic events.

5.7. Satellite disruption

Making rings by disrupting satellites naturally leads to consideration of the moons' evolution. The history of the small satellites of Uranus and Neptune has been studied in detail by

Colwell and Esposito (1992, 1993) and Colwell *et al* (2000). Their stochastic simulations of the moons' collisional fragmentation confirm the conclusions of Smith *et al* (1986, 1989) that these moons are not primordial. Table 3 gives estimated disruption lifetimes for small satellites of Uranus and Neptune. Many of these are significantly less than the age of the solar system. Different models for the strength in table 3 provide seriously different lifetimes (Colwell *et al* 2000), which do not allow a definitive history but give the general outline of destruction of small moons to make rings. Colwell and Esposito follow the process of satellite disruption from an initial distribution through successive disruptions, ignoring re-accretion. Two approaches are used: a Monte Carlo simulation following the history of only the largest fragment after each disruption, and a Markov chain calculation following the stochastic evolution of all the fragments (see section 6 for more discussion of this approach).

These simulations raise the question of re-accretion of fragments of a disrupted satellite in or near the planet's Roche zone. Previous estimates by Burns *et al* (1984) and Stevenson *et al* (1986) are based on the calculation of Soter (1971), who computed the timescale for an ejected particle to collide with its source body. Canup and Esposito (1995) have used a matrix formulation of the integro-differential coagulation equation and applied it to the ensemble of satellite fragments calculated by Colwell and Esposito (1992), to improve on Soter's (1971) calculation. This method was a particle-in-a-box simulation of the mutual collision statistics. Their results show that re-accretion should not be ignored: realistic calculations in the Roche zone must form a critical part of our understanding of ring and moon evolution. Already, we expect some limited re-accretion within rings as particles may temporarily stick together between higher velocity collisions. These temporary aggregations were termed *dynamic ephemeral bodies* (DEBs) by Weidenschilling *et al* (1984). Despite this proviso, the existence of rings surrounding the planets shows that accretion does not dominate near the planet, and the present models' general neglect of accretion in ring-history calculations seems justified.

Table 3. Estimated satellite disruption lifetimes for two strength models.

Satellite	Radius (km)	Orbit radius (10^4 km)	Disruption lifetime (10^9 years): Durda *et al* (1998)	Disruption lifetime (10^9 years): Housen *et al* (1991)
			Uranus	
Puck	77	8.60	56	4.0
Belinda	34	7.53	9.1	1.3
Rosalind	29	6.99	5.9	1.0
Portia	55	6.61	17	1.8
Juliet	42	6.44	10	1.3
Desdemona	29	6.27	5.0	0.83
Cressida	33	6.18	6.2	0.91
Bianca	22	5.92	2.9	0.59
Ophelia	16	5.38	1.4	0.38
Cordelia	13	4.98	0.91	0.29
			Neptune	
Proteus	208	11.76	1.2×10^4	25
Larissa	96	7.35	83	3.7
Galatea	79	6.19	29	2.3
Despina	74	5.25	20	1.7
Thalassa	40	5.01	5.9	0.83
Naiad	29	4.82	3.0	0.56

From Colwell *et al* (2000).

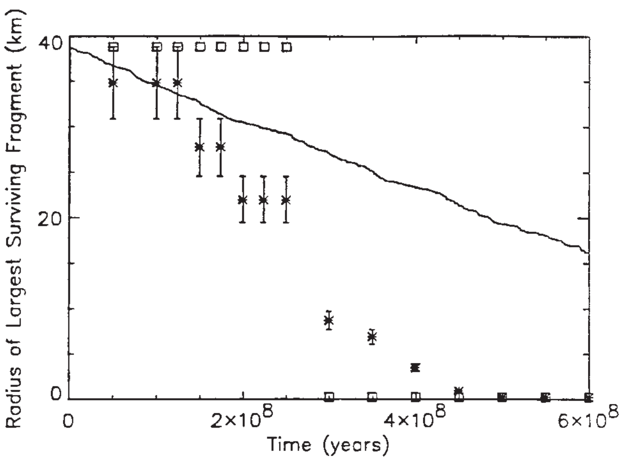

Figure 19. Mean (——), median (⋆) and modal (□) sizes of a distribution of 300 stochastic simulations of the collisional cascade for an initial 40 km radius moon, at the orbit of Thallassa. Error bars on the median connect the two size bins, which fall on either side of the 50% cumulative probability. From Colwell and Esposito (1992).

Once the original moon is destroyed for the first time, the collisional cascade to smaller size through successive disruptions occurs relatively quickly, since the smaller moons are easier to destroy. Monte Carlo simulations of 300 separate histories of the moons of Neptune give the results shown in figure 19. For an original moon of radius 40 km, the solid line shows the mean, asterisks the median, and squares the mode for the distribution of the largest surviving fragment as a function of time. These results show that the evolution of moon populations from catastrophic fragmentation is more complex than can be described by a simple timescale. The speed of this cascade is further dependent on the size distribution of the impactors, which is, unfortunately, a poorly known factor. For example, the difference between a power-law index of 2.5 and 3.5 is quite significant. Better constrained measurements of the impactor size distribution are strongly desired, although the most recent values do not change our conclusions significantly (Colwell *et al* 2000).

The Markov chain method (see section 6) follows the evolution of the complete size distribution of moons and fragments. These simulations show that the more numerous smaller fragments can outlive the largest fragment followed in the Monte Carlo formulation, yielding collisional debris from an initial complement of satellites that has an approximate power-law distribution. Colwell and Esposito (1992, 1993) find a cumulative-size power-law index of 2.54 for the collisionally evolved system. We note that after four billion years, the remnants of an original 100 km radius moon would include about 10^3 1–10 km moonlets.

The calculations of Colwell and Esposito (1992) and Colwell *et al* (2000) show that the small satellites of Neptune must have evolved through catastrophic fragmentation since the end of satellite and planet formation four billion years ago. The production of the currently observed smaller satellites is a natural consequence of the successive break-up of larger satellites.

5.8. Ring formation

Through further study of the size distribution and velocity distribution of the satellite fragments, Colwell and Esposito (1993) found that a narrow ring is the natural outcome of a disruption, as the fragments' orbits quickly fill the entire circumference at the original orbital radius of the destroyed moon. In the production of this debris, a small number of large fragments are also created. Colwell and Esposito (1990) argue that these larger fragments will naturally clear gaps. The discovery of Pan in Saturn's Encke Gap (Showalter 1991) may provide one example of this. As the initial ring spreads, its edges will cross through the resonances with larger bodies in the system, allowing the edges of the rings to be shepherded and sharpened. The moons will then spread with the rings (albeit more slowly because of the moons' larger mass), and possibly their evolving orbits will resonate with yet larger satellites. A natural result is that the evolved system will include many mutual resonances. This can explain the 'Cordelia connection' found by Murray and Thompson (1990) for the Uranus rings, i.e. that several of the unseen moons that are needed to halt the radial spreading of the Uranus rings are exceptionally close to resonances with Cordelia. Furthermore, they noted that Cordelia itself is very close to a resonance with Rosalind. This linking-up due to orbital resonances and associated transfer of angular momentum successively from smaller to more massive satellites will slow the initially rapid viscous spreading of the newly formed ring.

The moons can also confine the ring material in azimuth: Neptune's arcs provide a vivid example. Like the radial lock-up, this confinement occurs quite quickly; otherwise, differential rotation due to Kepler shear and differential precession would smear out the arcs on a timescale of years. Porco (1991) has shown how the azimuthal structure of the ring arcs may be understood as material trapped in 7 of 86 possible Galatea co-rotation resonances (see figure 20). All the ring arcs span an azimuthal range of only 25°; thus, the resonance locations are only thinly occupied.

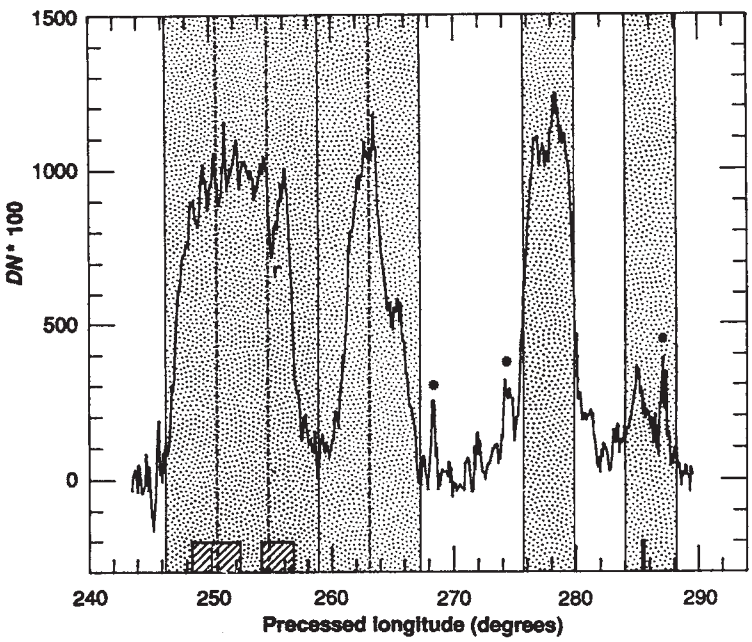

Figure 20. A radially averaged longitudinal scan of the arc region as seen in figure 16 and precessed back to a common epoch using the arcs' mean motion, $n = 820.118\,5°$ per day. The asterisks indicate the positions of stars; the symbol *r* indicates an incompletely removed camera reseau. The stippled bars show the location of co-rotation resonances, each 4.186° wide, which might explain the azimuthal confinement of the observed arcs in the model of Goldreich *et al* (1986). As can be seen, not all resonance zones are occupied by arcs, and some of the observed arcs fill more than one resonance. Reprinted with permission from Porco C C 1991 An explanation for Neptune's ring arcs *Science* **253** 995 ©1991 American Association for the Advancement of Science.

We can estimate the probability that Neptune's particular arrangement arose by a set of chance events (Esposito and Colwell 1992). One possibility is that each of the resonance locations was filled by an independent event. Examples might be a collision between two fast moving particles in one of the resonance zones, or the destruction of a small moon at or near the resonance site. Each event would release material to be subsequently trapped in that co-rotation resonance.

Esposito and Colwell find that the random hypothesis is excluded with a likelihood 1×10^{-8} (i.e. the probability of chance occurrence of all the ring arcs clustering together is 10^{-8}). The conclusion from this calculation is that we are most likely seeing the result of a single recent event. This could have been the collision of a meteoroid with a small moon of Neptune, resulting in the destruction of the moon; the smaller fragments would now be trapped in seven of the ten nearby co-rotation sites. This destruction could also simultaneously leave several large fragments (as explained above) to assist in the azimuthal confinement, as proposed in the model of Lissauer and Sicardy (1990).

5.9. Summary

Short lifetimes inferred from meteoroid bombardment imply interrelated histories for rings and nearby small moons in the planetary ring systems. Detailed simulations show the plausibility of a model where disrupted satellites provide the source of the Uranus and Neptune rings. The satellites confine the rings radially and azimuthally. The entire ring–moon system may lock up through resonances and evolve as a unit. Satellites excite the random motions within the rings. The resulting interparticle velocities determine the size distribution through collisional equilibrium. The collisions also produce the significant amounts of dust observed by the Voyager cameras in the Uranus and Neptune rings.

6. Stochastic models of planetary rings

6.1. Motivation

Models of ring dynamics and history are most often deterministic. The dynamical model can be a numerical simulation that explicitly solves a differential equation. Alternatively, each particle in the simulation is followed (this is the *N-body simulation*, where a set of N particles provides a sample of the ring evolution). Stewart *et al* (1984) review kinetic approaches. Recent examples of N-body simulations are by Salo (1995) and Lewis and Stewart (2002). These models, although often idealized and simulating a limited time interval, clearly explicate the ring evolution. Nonetheless, it is clear that random events have played a significant role in the history of planetary rings. This goes beyond the normal fluctuations about the mean that are characteristic of other truly random processes such as diffusion in a gas (see, e.g. Landau and Lifshitz (1969) volume 5, chapter 10). The importance of stochastic processes for rings is not just the random nature of the significant evolutionary events but the fact that the present nature of planetary rings is dominated by just a small number of recent events.

The contingency on a few random events may explain why each planet's ring systems appear different. A small number of larger bodies may dominate the mass, history, and dynamics of ring systems. The rings themselves are likely the progeny of singular events like the destruction of a former moon or of a comet that passed too close. In the continuing competition between fragmentation and accretion, occasional major events set the pace. Transient features like arcs, clumps, and spokes are common. Altogether, ring history seems disorderly: rings display little of the Newtonian clockwork and clarity we often associate with the heavens.

These aspects of planetary rings mean that, often, we must account for random events and their ramifications in ring history. An approach continuous in time and space may overlook the jagged nature of the phenomenon. Furthermore, the present state of the rings is contingent on these past events: the details of each particular history cannot be ignored. The rings' current state may be just a particular sample that nature has drawn at random from a large range of similar (or perhaps dissimilar) possible outcomes. Thus, when we explain the ring observations, we must not only match what we see but also consider the likelihood of the particular outcome we observe.

My approach to handling these aspects is to consider ring dynamics and history as stochastic processes, that is, physical processes that are subject to random events and that evolve probabilistically in time. I briefly describe some useful concepts below.

6.2. *Stochastic processes*

The general idea of a stochastic process is a (discrete or continuous) sequence of random variables $X_i(t_n)$ (continuous $X_i(t)$). These X_i are the numerical outcomes of the random events in the system and thus represent the values of some physical parameters of interest at times t_n (continuous: t). The random variables X_i have a probability distribution at time t_n that may depend on the past history of the system. A *stochastic process* is the mathematical abstraction of an empirical process whose development is governed by probabilistic laws.

6.3. *Random walk on the line*

As an example, consider a particle on the origin of the Cartesian x-axis. At constant intervals, it moves unit distance, either right or left, with probability p or q, respectively ($p + q = 1$). This stochastic process, called the *random walk* (and sometimes the *drunkard's walk*), is an analogue for the physical processes of Brownian motion and diffusion. If $p = q = \frac{1}{2}$, the walk is symmetric; for $p > q$, the process shows a drift to the right. In such a drunkard's walk, each step is independent, that is, p and q do not depend on time or the drunk's current position.

6.4. *Markov processes*

The idea of a Markov process generalizes this idea of independence. For a Markov process, the conditional probabilities at a time t_n depend only on the state of the system at the time t_n and not on its previous history. The *Markov process* is a particular type of stochastic process that lends itself readily to linear algebra and matrices (see Kemeny and Snell (1960), Esposito and House (1978)). The great value of Markov processes is that they are not only simply handled mathematically but they are also applicable to many practical problems, including the evolution of planetary rings. A finite Markov chain has a finite number of values of the random variable corresponding to discrete states of a physical system. At discrete time intervals, the physical system transitions to its next state (i.e. the value of the random variable at the next time step). The probabilities for this transition depend only on the current state (this independence is the *Markov property*) and are independent of time. In this case, the state of the system is described by a *state vector* at any time (including, for example, the initial state, representing the initial conditions), and the transition probabilities can be arranged as a matrix. Successive multiplications of the state vector by the *transition matrix* gives the probabilistic evolution of the system with time. The state vector gives the expectation value for all the possible (finite) states of the system as the system evolves. This approach can be used even where a deterministic approach would also suffice. In Canup and Esposito (1995, 1997), we modelled the accretional growth of small bodies in the Roche zone with a Markov process that is entirely equivalent to solving the integro-differential equation for accretion. Brophy and Esposito (1989) modelled the collisional dynamics of narrow rings with a finite Markov chain: since this could also be cast as an N-body calculation or the solution of the Boltzmann equations for the kinetic ring system (see Stewart *et al* (1984)), the benefits were purely practical. It was convenient for us to ignore the details of individual orbits and collisions and take a statistical approach using this formulation. If the motion of ring particles is chaotic, as for example in Neptune's rings (Foryta and Sicardy 1995), this is a natural approach (Esposito *et al* 1996).

6.5. Markov chains and Monte Carlo simulations

Another way to simulate the evolution of a probabilistic system is to draw random numbers that determine the successive states of the stochastic process at each time step. This is called the *Monte Carlo* method. If the random numbers are drawn against the conditional probabilities for a Markov chain, the state vectors calculated by successive multiplications give the expectation values for the Monte Carlo simulations after each step: thus, the two methods are equivalent for the discrete-time, *discretized* (finite number of states) system. The Monte Carlo method gives a particular actualization of one possible history of the stochastic process. My students and I refer to this as 'watching the video' of the Markov chain. If we are concerned with singular events, or outcomes with small-numbers statistics, then the Monte Carlo simulation is what should be directly compared to our observations of planetary rings (see Colwell and Esposito (1992)).

6.6. Stochastic processes as ring models

Several good reasons justify using stochastic models. First, the actual physical processes are stochastic. In planetary rings, collisions, resonance trapping and escape, charging of dust by individual electrons, accretion, and fragmentation are all random events. Second, analytic solutions often do not exist and the partial differential equations may be difficult to solve. In this case, the stochastic models provide a numerically robust method for tracking the evolution of the system. Third, stochastic models simulate the actual time history (i.e. the 'video') of systems that may be far from equilibrium and subject to singular events. Fourth, the probabilistic methods have a simple physical interpretation as the evolution of the state distribution of the key physical variables. It is easy to understand the results. Fifth, this approach emphasizes the contingent nature of the results. Each particular outcome is associated with its probability of occurrence. Every history may be different. In particular cases, the dynamics are dominated by a limited number of the most massive bodies in the ensemble.

The stochastic approach can thus accommodate aspects of evolution that are difficult for a classical 'clockwork' approach, for example, chaotic dynamics and catastrophic events. This is true when large fluctuations or jumps occur, e.g. birth and death processes for small numbers. Röpke (1987) remarks that the deterministic transport equation like the Liouville equation is just a 'degenerate' Markov process: the outcome is completely determined. Where small numbers dominate, as in the collisional cascade to form rings (Colwell and Esposito 1992, 1993) or the sudden brightenings of Saturn's F ring (Barbara and Esposito 2002), the stochastic approach can capture these aspects. This emphasizes the contingency of the present state: it depends on a few random events. In the case of ring evolution, these are, for example, how many satellites, how close to the Roche limit, and what was the most recent catastrophic destruction. This contingency provides a philosophical connection to the current understanding of the demise of the dinosaurs or the formation of our Moon. Our present Moon and our present human dominance are contingent on rare, chance events like those that create planetary rings. In all these cases, the actual histories bear little relation to the ensemble averages. Our stochastic models, beyond their ease and practical advantages, capture essential aspects of our solar system.

7. The big questions

Of course, every new discovery leads to new questions. Our recent progress in understanding their physics leads naturally to several major open questions about planetary rings, as follows.

7.1. Origin and evolution

Just how old are the rings, where did they come from, and what is their future? Can we solidify the genetic relation between moons and rings? What is the contribution of external factors like meteoroid bombardment to ring history? Did the Earth ever possess a ring, perhaps as an intermediate stage in forming our Moon?

7.2. Ring make-up

What are the chemical composition, size distribution, and shape of the ring particles? How do these aspects combine to give the rings' appearance and other characteristics visible at a distance? Can we have a close-up view of individual ring particles?

7.3. Origins of planets

Obviously, the rings preserve some part of the history of their own planet and its system of satellites. How can we read this information? Will detailed study of ring dynamics clarify the processes that occur when a disk around a star coalesces to form planets? The rings we see are cold, with frequent collisions and large opacity; they exist in the region where the tides from the primary act to retard accretion (the *Roche zone*). These aspects are all different from the planet-forming environment. Despite these limitations, the rings show the effects of embedded large bodies, chaotic interactions, and azimuthally nonsymmetric effects like bending waves and warps. These phenomena are important in forming planets.

Furthermore, our experience is that answering the questions raised by explaining the real phenomena in planetary rings has stretched the existing theoretical and numerical methods. These improved methods have then been applied to other disk systems. This application of ring studies to understanding how planets form may be the largest pay-off of ring research.

To answer the above questions, no single finding or measurement will suffice. In-depth, multi-instrument observations and linked theoretical developments are required. A particular opportunity is now provided by the joint NASA–ESA Cassini mission.

8. Future ring observations by Cassini

The Cassini orbiter is now on its way to Saturn, to arrive in July 2004 and orbit the planet for at least four years. On the way, it flew by Jupiter in December 2000, providing a distant view of that planet, its moons, and its rings. The planned observations are described in a review by Cuzzi *et al* (2001). I will briefly summarize the spacecraft capability and objectives.

The Voyager fly-bys of the 1980s changed forever how we think about planetary rings. Cuzzi (1998) describes this as a ‘paradigm shift’ that led us to the current conception of young and dynamic rings. The new and exotic phenomena seen close-up by the Voyager spacecraft forced us to expand our conceptions and adjust them to the immediate reality. Unfortunately, the Voyager investigations were spotty in coverage, both in time and space, with limited images and only a few wavelengths. The Cassini spacecraft benefits from the capability of experiments developed one generation later, and further from the long duration of its planned four-year tour of the Saturn system. This duration allows us to address new questions and phenomena as they arise, and to follow up with deeper investigations. We will also track the evolution of singular events in Saturn’s rings that occur during the mission. Some tantalizing ‘bright clumps’ seen by Voyager in Saturn’s F ring (Showalter 1998) provide one example of targets for monitoring by Cassini’s cameras.

The Cassini capability exceeds that of Voyager in every area. The cameras will resolve sub-kilometre structure in the rings. Multiday ‘movies’ will track spokes, F-ring phenomena, and small satellites. Up to 100 stellar and solar occultations will define the radial and azimuthal structure in the rings, resolving many as small as tens of metres (Esposito *et al* (1998); see figures 21 and 22). The Cassini experiments will observe the rings at wavelengths from the extreme UV to the mid-IR. Radio occultations will define the particle size distribution for particles whose size ranges from millimetres to tens of metres. The Cassini orbit will provide a full range of observing geometry to catch the lit, unlit, shadowed, backlit, and full-phase (when the sun is directly behind the spacecraft) rings. The combination of observing over this range of wavelengths and angles will give a complete picture of the vertical structure, particle

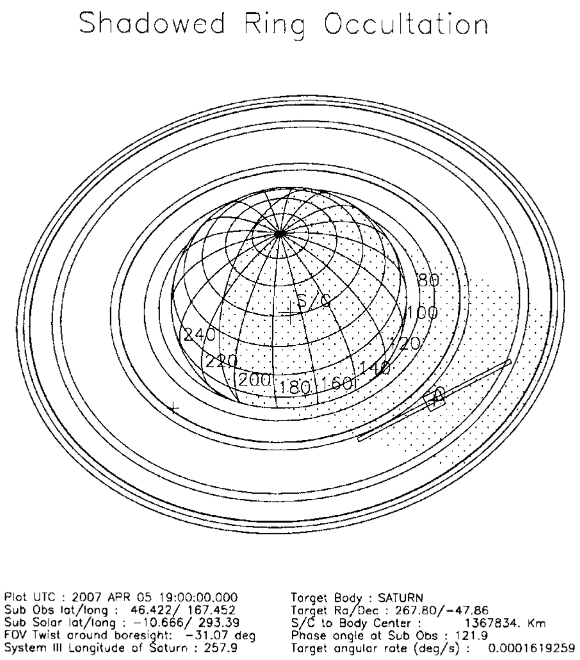

Figure 21. The star ε Canum Majoris occulted by the shadowed rings of Saturn during the Cassini orbital tour on 24 and 25 October 2001. The Cassini UVIS far-ultraviolet occultation slit (long rectangle) and high-speed photometer aperture (small square) are shown. Stippling indicates shadowed regions of the planet and rings. After Esposito *et al* (1998).

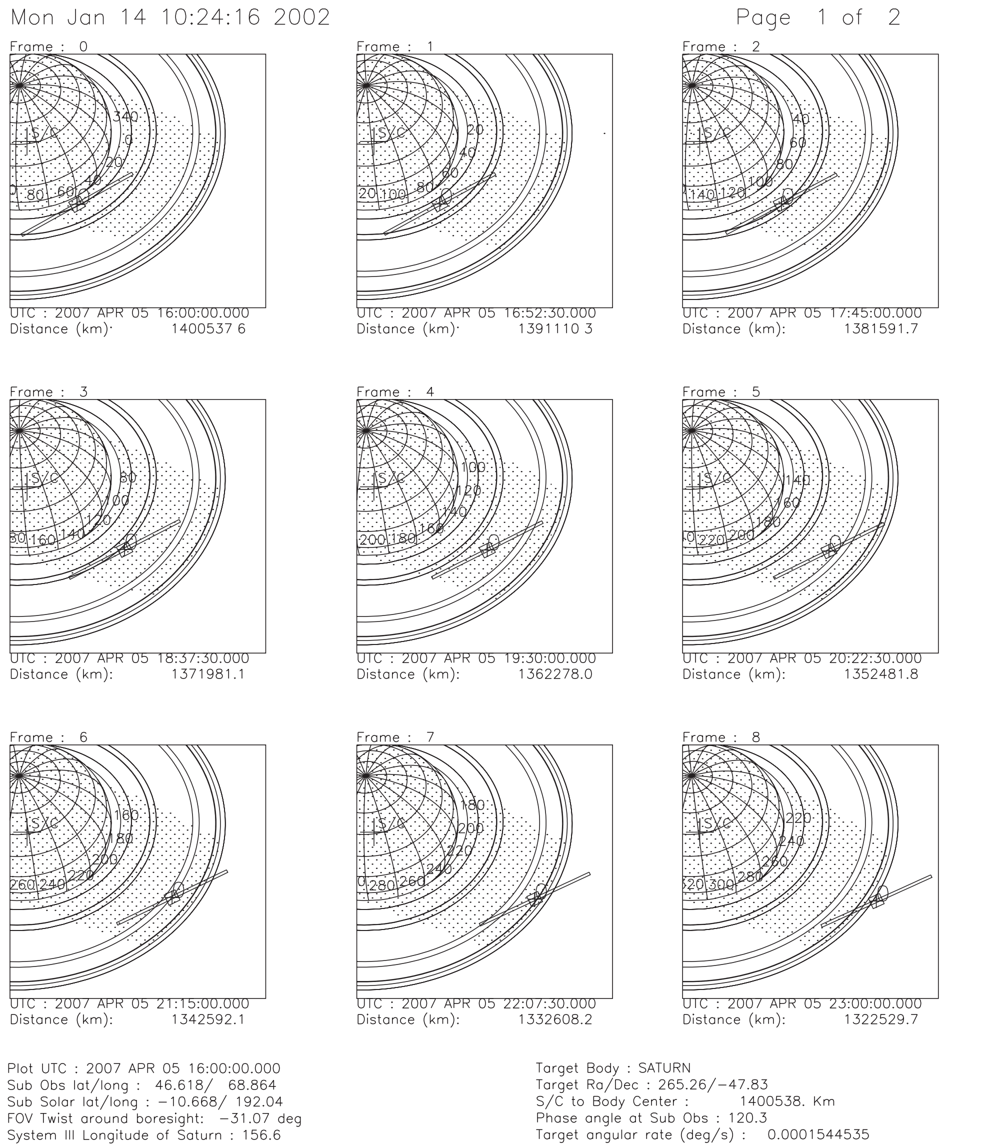

Figure 22. An animated sequence of a stellar occultation across the shadowed rings with viewing geometry similar to figure 21. The duration of the occultation is approximately 2.5 h. After Esposito *et al* (1998).

temperatures, and shapes. Multiple observations will catch waves and wakes in action. The orbiter will measure the dust in the diffuse rings, around the rings, and in the bombarding meteorite population. The comprehensive Cassini payload will characterize the interactions of rings, atmosphere, ionosphere, and magnetosphere as well as ring–satellite relations and ring evolution (Cuzzi *et al* 2001). Joseph Burns of Cornell University says that 'Cassini results may fundamentally alter our understanding of ring processes and even origins.'

The most critical observations (close-ups, movies, radio and stellar occultations, dark-side and back-side views) cannot be achieved from Earth. The comprehensive payload of science instruments provides overlapping and mutually reinforcing measurements that can answer many of the current questions and also address the new discoveries that arise. Cassini will be able to follow up on episodic or rare phenomena it observes in the ring system and track their effects.

As an example, two satellites of Saturn, Janus and Epimetheus, share nearly the same orbit and every four years at their closest approach, they exchange angular momentum and switch orbits. For the following four years, the other satellite is the inner one, then they switch again! All the waves they excite at ring resonances will also suddenly adjust (Murray 1994). Cassini will have the opportunity to observe this switch and its effects during its orbital tour, along with close encounters between satellites and rings and the slow outward evolution of the ringmoons.

Fortunately for Cassini, the spacecraft has no plans to crash into the rings. Even small particles of one millimetre or so can be deadly, but they are likely to be rare outside the visible rings (Canup and Esposito 1997). Unfortunately, this means that we will attain no close-up views of individual ring particles. NASA now has plans for a future 'Ring Observer' mission that would come close enough to the rings to hover and capture pictures of the individual particles. Such views would provide spectacular 'ground truth' for the remote sensing from fly-by and orbiter spacecraft.

9. Conclusions

Our present understanding of planetary rings highlights a number of important scientific questions. One question is to explain the visible differences between the several planetary ring systems (my proposal is that these differences represent different random outcomes of the same stochastic processes of ring creation and destruction). Further, our description of the various ring systems is still incomplete, especially knowledge of the complete size distribution and the composition of the ring particles (which, in fact, may vary within each system). In addition, we need to measure accurately the locations of the rings and their three-dimensional structure. Present theoretical models of ring dynamics should be compared in detail with the best measurements in order to test and refine our explanations.

The questions of the age of the rings, their recent origins, and their history have been brought into sharp focus by spacecraft observations of many youthful features and by calculations that the present rings could not have persisted for the age of the solar system. The rings thus are subject to a combination of transient and confining processes. Perhaps the most important question is how our understanding of present processes in planetary rings can be fruitfully compared with those in the early solar nebula to explain the origin of the planets out of a flat disk of interacting particles, dust, and gas. We could then apply this understanding to other flattened, rotating systems like galaxies and accretion disks.

Our current understanding of planetary rings leads to several major measurement objectives. The first is to measure radial, azimuthal, and vertical structure at high spatial resolution and multiple times. This involves not only high-resolution imaging and radio, stellar, and solar occultations from planetary orbits, which can be provided for the Jupiter rings by the NASA Galileo mission and for Saturn's rings by the NASA/ESA Cassini mission, but also full utilization of ground-based stellar occultations.

The second goal is to measure the complete size distribution and composition of the ring systems at multiple locations, from the smallest transient dust particles up to the embedded moons within and near the ring system. Space missions like Cassini, using radio occultation, spectroscopy, and photometric measurements can meet this objective.

The third objective is to develop models of ring processes and history that are consistent with the best Earth and space observations and establish the rings' relation to moons, atmospheres, and magnetospheres in their planetary systems and to the early solar system. This development will depend on a better description from future spacecraft and Earth-based data and will provide a direct benefit to our understanding of the origin of the solar system. These advances all involve close collaboration between the observers and the model developers. The explosion of our understanding of planetary rings in the last two decades shows the power of such a combined approach.

Acknowledgments

I appreciate helpful discussions with Glen Stewart, Tom Brophy, Robin Canup, Mihaly Horanyi, Mark Lewis, Joshua Colwell, Shawn Brooks, and Andre Brahic. I thank Juergen Schmidt, Frank Spahn, and Alexander Krivov for their comments on this manuscript, and David Stevenson for a constructive review. I thank the NASA Planetary Geology Program and Outer Planets Data Analysis Program, the Jupiter System Data Analysis Program, and the Voyager, Galileo, and Cassini projects for support of this research.

References

Araki S and Tremaine S D 1986 The dynamics of dense particle disks *Icarus* **65** 83–109

Barbara J M and Esposito L W 2002 Moonlet collisions and the effects of tidally modified accretion in Saturn's F ring *Icarus* at press

Baum, W A, Kreidl T, Westphal J A, Danielson G E, Seidelmann P K and Pascu D 1981 Saturn's E-ring I. CCD observations of March 1980 *Icarus* **47** 84–96

Borderies N, Goldreich P and Tremaine S 1989 The formation of sharp edges in planetary rings by nearby satellites *Icarus* **80** 344–60

Borderies N P, Goldreich P and Tremaine S D 1984 Unsolved problems in planetary rings dynamics *Planetary Rings* ed R Greenberg and A Brahic (Tucson: University of Arizona Press) pp 713–36

Borderies N P, Goldreich P and Tremaine S D 1985 A granular flow model for dense planetary rings *Icarus* **63** 406–20

Bosh A S, Olkin C B, French R G and Nicholson P D 2002 Saturn's F ring: kinematics and particle sizes from stellar occultation studies *Icarus* **157** 57–75

Brahic A 1975 A numerical study of a gravitating system of colliding particles: applications to the dynamics of Saturn's rings and to the formation of the solar system *Icarus* **25** 452–8

Brahic A 1977 Systems of colliding bodies in a gravitational field: numerical simulation of the standard model *Astron. Astrophys.* **54** 895–907

Brooks S and Esposito L W 2000 Photometry of Jupiter's main ring with Galileo SSI and NIMS imaging. Paper presented at the *Lunar and Planetary Science Conf. (Houston)*

Brooks S, Esposito L W, Throop H B and Showalter M R 2002 Photometric analysis of Jupiter's main ring with Galileo SSI and NIMS imaging. Paper presented at the *International Jupiter Conf. (Boulder)*

Brophy T G and Esposito L W 1989 Simulation of collisional transport processes and the stability of planetary rings *Icarus* **78** 181–205

Brophy T G, Stewart G R and Esposito L W 1990 A phase-space fluid simulation of a two-component narrow planetary ring: particle size segregation, edge formation, and spreading rates *Icarus* **83** 133–55

Brophy T G, Esposito L W, Stewart G R and Rosen P D 1992 Numerical simulation of satellite–ring interactions: resonances and satellite-ring torques *Icarus* **100** 412–33

Burns J A, Showalter M R, Cuzzi J N and Pollack J B 1980 Physical processes in Jupiter's ring: clues to its origin by Jove! *Icarus* **44** 339–60

Burns J A, Showalter M R and Morfill G E 1984 The ethereal rings of Jupiter and Saturn *Planetary Rings* ed R Greenberg and A Brahic (Tucson: University of Arizona Press) pp 200–72

Burns J A, Hamilton D P, Showalter M R, Nicholson P D, de Pater I, Ockert-Bell M E and Thomas P C 1999 The formation of Jupiter's faint rings *Science* **284** 1446–50

Burns J A, Hamilton D P and Showalter M R 2001 Dusty rings and circumplanetary dust: observations and simple physics *Interplanetary Dust* ed E Grun, B A S Gustafson, S F Dermott and H Fechtig (Berlin: Springer) pp 641–725

Burns J A, Hamilton D P and Showalter M R 2002 Bejeweled worlds *Sci. Am.* **286** 64–73

Camichel H 1958 Mesures photométriques de Saturne et son anneau *Ann. Astrophys.* **21** 231–42

Canup M and Esposito L W 1992 Reaccretion of disrupted planetary satellites. Paper presented at the *AAS Division of Planetary Sciences Meeting (Munich)*

Canup R M and Esposito L W 1995 Accretion in the Roche zone: coexistence of rings and ringmoons *Icarus* **113** 331–52

Canup R M and Esposito L W 1997 Evolution of the G ring and the ring hazard to Cassini *Icarus* **126** 28–41

Chiang E I and Goldreich P 2001 Apse alignment of narrow eccentric planetary rings *Astrophys. J.* **540** 1084–90

Colwell J E and Esposito L W 1990a A numerical model of the Uranian dust rings *Icarus* **86** 530–60

Colwell J E and Esposito L W 1990b A model of dust production in the Neptune ring system *Geophys. Res. Lett.* **17** 1741–4

Colwell J E and Esposito L W 1992 Origins of the rings of Uranus and Neptune I. Statistics of satellite disruptions *J. Geophys. Res.* **97** 10,227–41

Colwell J E and Esposito L W 1993 Origins of the rings of Uranus and Neptune II. Initial distributions of disrupted satellite fragments *J. Geophys. Res. (Planets)* **98** 7387–401

Colwell J E, Esposito L W and Bundy D 2000 Fragmentation rates of small satellites in the outer solar system *J. Geophys. Res.* **105** 17,589–99

Cook A F and Franklin F A 1964 Rediscussion of Maxwell's Adams prize essay on the stability of Saturn's rings *Astron. J.* **69** 173–200

Cooke M L 1991 Radial variation in the Keeler Gap and C ring photometry *PhD Thesis* Cornell University

Cuzzi J N 1995 Evolution of planetary ringmoon systems *Earth, Moon, and Planets* **67** 179–208

Cuzzi J N 1998 Ringside seat *The Sciences* **38** 28–33

Cuzzi J N and Burns J A 1988 Charged particle depletion surrounding Saturn's F ring: evidence for a moonlet belt? *Icarus* **74** 284–324

Cuzzi J N and Durisen R H 1990 Bombardment of planetary rings by meteoroids: general formulation and effects of Oort cloud projectiles *Icarus* **84** 467–501

Cuzzi J N and Esposito L W 1987 The rings of Uranus *Sci. Am.* **237** 52–66

Cuzzi J N, Lissauer J J, Esposito L W, Holberg J B, Marouf E A, Tyler G L and Boischot A 1984 Saturn's rings: properties and processes *Planetary Rings* ed R Greenberg and A Brahic (Tucson: University of Arizona Press) pp 73–199

Cuzzi J N, Colwell J E, Esposito L W, Porco C C, Murray C E, Nicholson P D, Spilker L J, Marouf E A, French R G and Rappaport N 2001 Saturn's rings: pre-Cassini status and mission goals 2002 *Sp. Sci. Rev.* at press

Daisaka H, Tanaka H and Ida S 2002 Viscosity in a dense planetary ring with self-gravitating particles *Icarus* **154** 296–312

de Pater I and Lissauer J J 2001 *Planetary Sciences* 11. Planetary rings (Cambridge: Cambridge University Press) pp 403–36

Dermott S 1984 Dynamics of narrow rings *Planetary Rings* ed R Greenberg and A Brahic (Tucson: University of Arizona Press) pp 589–640

Dollfus A 1970 Optical reflectance polarimetry of Saturn's globe and rings *Icarus* **40** 171–9

Dones L R 1987 Dynamical and photometric studies of Saturn's rings *PhD Thesis* University of California, Berkeley

Dones L R 1991 A recent cometary origin for Saturn's rings? *Icarus* **92** 194–203

Dones L R, Showalter M R and Cuzzi J N 1989 Simulations of light scattering in planetary rings *Dynamics of Astrophysical Disks* ed J Sellwood (Cambridge: Cambridge University Press) pp 25–6

Doyle L R and Grün E 1990 Radiative transfer modelling constraints on the size of spoke particles in Saturn's rings *Icarus* **85** 168–90

Doyle L R, Dones, L and Cuzzi J C 1989 Radiative transfer modelling of Saturn's outer B ring *Icarus* **80** 104–35

Dumas C, Terrile R T, Smith B A, Schneider G and Becklin E E 1999 Stability of Neptune's ring arcs in question *Nature* **400** 733–5

Durda D D, Greenberg R and Jedicke R 1998 Collisional models and scaling laws: a new interpretation of the shape of the main-belt asteroid size distribution *Icarus* **135** 431–40

Durisen R H, Cramer N L, Murphy B W, Cuzzi J N, Mullikin T L and Cederbloom S E 1989 Ballistic transport in planetary ring systems due to particle erosion mechanisms I. Theory, numerical methods, and illustrative examples *Icarus* **80** 136–66

Durisen R H, Bode P W, Cuzzi J N, Cederbloom S E and Murphy B W 1992 Ballistic transport in planetary ring systems due to particle erosion mechanisms II. Theoretical models for Saturn's A- and B-ring inner edges *Icarus* **100** 364–93

Durisen R H, Bode P W, Dyck S G, Cuzzi J N, Dull J D and White J C III 1996 Ballistic transport in planetary ring systems due to particle erosion mechanisms III. Torques and mass loading by meteoroid impacts *Icarus* **124** 220–36

Elliot J L, Dunham E W and Mink D J 1977 The rings of Uranus *Nature* **267** 328–30

Elliot J L, French R G, Frogel J A, Elias J H, Mink D J and Liller W 1981 Orbits of the nine Uranian rings *Astron. J.* **86** 444–55

Elliot J L *et al* 1985 The 1983 June 15 occultation by Neptune I. Limits on a possible ring system *Astron. J.* **90** 2615–23

Eplee R E and Smith B A 1987 A dynamical constraint on particulate sizes for Saturn's B ring spokes *Icarus* **69** 575–7

Esposito L W 1986 Structure and evolution of Saturn's rings *Icarus* **67** 345–57

Esposito L W 1993 Understanding planetary rings *Ann. Rev. Earth and Plan. Sci.* **21** 487–523

Esposito L W and Colwell J E 1989 Creation of the Uranus rings and dust bands *Nature* **339** 637–740

Esposito L W and Colwell J E 1992 Neptune's rings and satellite system: collisional origin and evolution. Paper presented at the *American Geophysical Union Meeting (Montreal)*

Esposito L W and House L L 1978 Radiative transfer calculated from a Markov-chain formalism *Astrophys. J.* **219** 1058–67

Esposito L W, Dilley J P and Fountain J W 1980 Photometry and polarimetry of Saturn's rings from Pioneer 11 *J. Geophys. Res.* **85** 5948–56

Esposito L W, O'Callaghan M and West R A 1983a The structure of Saturn's rings: implications from the Voyager stellar occultation *Icarus* **56** 439–52

Esposito L W, O'Callaghan M, West R A, Hord C W, Simmons K E, Lane, A L, Pomphrey R B, Coffeen D L and Sato M 1983b Voyager PPS stellar occultation of Saturn's ring *J. Geophys. Res.* **88** 8643–9

Esposito L W, Cuzzi J N, Holberg J B, Marouf E A, Tyler G L and Porco C C 1984 Saturn's rings: structure, dynamics and particle properties *Saturn* ed T Gehrels and M S Matthews (Tucson: University of Arizona Press) pp 463–545

Esposito L W, Brahic A, Burns J A and Marouf E A 1991 Particle properties and processes in Uranus' rings *Uranus* ed J T Bergstralh, E D Miner and M S Matthews (Tucson: University of Arizona Press) pp 410–68

Esposito L W, Colwell J E and Canup R M 1996 History of Neptune's ring arcs *Bull. Am. Astron. Soc. 29th DPS Meeting Abstracts* **29** 1000

Esposito L W, Colwell J E and McClintock W E 1998 Cassini UVIS observations of Saturn's rings *Planet. Space. Sci.* **46** 1221–35

Foryta D W and Sicardy B 1996 The dynamics of the Neptunian Adams ring's arcs *Icarus* **123** 129

French R G and Nicholson P D 2000 Saturn's rings II. Particle sizes inferred from stellar occultation data *Icarus* **145** 502–23

French R G, Elliot J L and Levine S E 1986 Structure of the Uranian rings II. Ring orbits and widths *Icarus* **67** 134–63

French R G, Nicholson P D, Porco C C and Marouf E A 1991 Dynamics and structure of the Uranian rings *Uranus* ed J T Bergstralh, E D Miner and M S Matthews (Tucson: University of Arizona Press) pp 410–68

French R G, McGhee C A, Nicholson P D, Dones L and Lissauer J J 1999 Saturn's wayward shepherds. Paper presented at *AAS Division of Dynamical Astronomy Meeting (Estes Park)*

Gehrels T *et al* 1980 Imaging photopolarimeter on Pioneer Saturn *Science* **207** 434–9

Goldreich P and Porco C C 1987 The shepherding of the Uranus rings II. Dynamics *Astron. J.* **93** 730–7

Goldreich P and Tremaine S 1978a The velocity dispersion in Saturn's rings *Icarus* **34** 227–39

Goldreich P and Tremaine S 1978b The formation of the Cassini Division in Saturn's rings *Icarus* **34** 240–53

Goldreich P and Tremaine S D 1979 Towards a theory for the Uranian rings *Nature* **277** 97–9

Goldreich P and Tremaine S D 1980 Disk–satellite interactions *Astrophys. J.* **241** 425–41

Goldreich P and Tremaine S D 1982 The dynamics of planetary rings *Ann Rev. Astron. Astrophys.* **20** 249–83

Goldreich P, Tremaine S and Borderies N 1986 Toward a theory for Neptune's arc rings *Astron. J.* **92** 195–8

Greenberg R 1983 The role of dissipation in the shepherding of ring particles *Icarus* **53** 207–18

Gresh D L 1990 Voyager radio occultation by the Uranian rings: structure, dynamics and particle size *PhD Thesis* Stanford University

Gresh D L, Marouf E A, Tyler G L, Rosen P A and Simpson R A 1989 Voyager radio occultation by Uranus's rings I. Observational results *Icarus* **78** 131–68

Grün E, Morfill G E and Mendis D A 1984 Dust-magnetosphere interactions *Planetary Rings* ed R Greenberg and A Brahic (Tucson: University of Arizona Press) pp 275–332

Hamilton D P and Burns J A 1994 Origin of Saturn's E ring: self-sustained, naturally *Science* **262** 550–3

Hammeen-Anttila K A 1978 An improved and generalized theory for the collisional evolution of Keplerian systems *Astrophys. Space Sci.* **58** 477–519

Harris A W 1984 The origin and evolution of planetary rings *Planetary Rings* ed R Greenberg and R Brahic (Tucson: University of Arizona Press) pp 641–59

Holberg J B, Forester W and Lissauer J J 1982 Identification of resonance features within the rings of Saturn *Nature* **297** 115–20

Holberg J B, Nicholson P D, French R G and Elliot J L 1987 Stellar occultation probes of the Uranian rings: a comparison of Voyager UVS and Earth-based results *Astron. J.* **94** 178–88

Horanyi M 1998 Dust plasma interactions at Jupiter *Astrophys. Space Sci.* **264** 257–71

Horn L J, Yanamandra-Fisher P A, Esposito L W and Lane A L 1989 Physical properties of the Uranian delta ring from a possible density wave *Icarus* **76** 485–92
Housen K R and Holsapple K A 1990 On the fragmentation of asteroids and planetary satellites *Icarus* **84** 226–53
Housen K R, Schmidt R M and Holsapple K A 1991 Laboratory simulations of large scale fragmentation events *Icarus* **94** 180–90
Ip W-H 1988 An evaluation of a catastrophic fragmentation origin of the Saturnian ring system *Astron. Astrophys.* **199** 340–2
Juhasz A and Horanyi M 2002 Saturn's E ring: a dynamical approach *J. Geophys. Res.* **107** 1029
Kemeny J and Snell J 1960 *Finite Markov Chains* (Princeton: Van Nostrand)
Kolvoord R A and Burns J A 1992 Three-dimensional perturbations of particles in a narrow planetary ring *Icarus* **95** 253–64
Kolvoord R A, Burns J A and Showalter M R 1990 Periodic features in Saturn's F ring *Nature* **345** 675–7
Landau L and Lifshitz E M 1969 *Statistical Physics* vol 5 (Menlo Park: Addison-Wesley)
Lane A L, Hord C W, West R A, Esposito L W, Coffeen D L, Sato M, Simmons K E, Pomphrey R B and Morris R B 1982 Photopolarimetry from Voyager 2: preliminary results on Saturn, Titan, and the rings *Science* **215** 537–43
Lewis M D 2001 Dynamics of strongly perturbed planetary rings *PhD Thesis* University of Colorado, Boulder
Lewis M D and Stewart G R 2000 Collisional dynamics of perturbed planetary rings *Astronom. J.* **120** 3295–310
Lin D N C and Bodenheimer P 1981 On the stability of Saturn's rings *Astrophys. J.* **248** L83–6
Lin D N C and Papaloizou J 1979 Tidal torques on accretion disks in binary systems with extreme mass ratios *Mon. Not. Roy. Astr. Soc.* **186** 799–812
Lissauer J J and Sicardy B 1990 Models of arcs in Neptune's 63K ring. Paper presented at *23rd COSPAR Meeting (Hague, Netherlands)*
Lissauer J J, Squyres S W and Hartmann W K 1988 Bombardment history of the Saturn system *J. Geophys. Res.* **93** 13776–804
Longaretti P-Y and Borderies N 1986 Non-linear study of the Mimas 5 : 3 density wave *Icarus* **67** 211–33
Lumme K A and Irvine W M 1979 A model for the azimuthal brightness variations in Saturn's rings *Nature* **282** 695–6
Lumme K A, Esposito L W, Irvine W M and Baum W A 1977 Azimuthal brightness variations of Saturn's rings II. Observations at an intermediate tilt angle *Astrophys. J.* **216** L123–6
Lynden-Bell D and Pringle J E 1974 The evolution of viscous discs and the origin of the nebular variables *Mon. Not. Roy. Astr. Soc.* **168** 603–37
McMuldroch S M, Pilorz S H and Danielson G E 1999 Galileo NIMS near-IR observations of Jupiter's ring system *Icarus* **146** 1–11
Meyer-Vernet N and Sicardy B 1984 On the physics of resonant disk-satellite interaction *Icarus* **69** 157–75
Mignard F 1984 Effects of radiation forces on dust particles *Planetary Rings* ed R Greenberg and A Brahic (Tucson: University of Arizona Press) pp 333–66
Morfill G E, Fechtig H, Grün E and Goertz C K 1983a Some consequences of meteoroid impacts on Saturn's ring *Icarus* **55** 439–47
Morfill G E, Grün E, Johnson T V and Goertz C K 1983b On the evolution of Saturn's spokes: theory *Icarus* **53** 230–5
Murray C D and Thompson R P 1990 Orbits of shepherd satellites deduced from the structure of the rings of Uranus *Nature* **348** 499–502
Murray C D, Gordon M K and Giuliatti-Winter S M 1997 Unraveling the strands of Saturn's F ring *Icarus* **129** 304–16
Namouni F and Porco C 2002 The confinement of Neptune's ring arcs by the moon Galatea *Nature* **417** 45–7
Nicholson P D and Dones L 1991 Planetary Rings *Rev. Geophys.* **29** (suppl) 313–27
Nicholson P D, Cooke M L, Matthews K, Elias J and Gilmore G 1990 Five stellar occultations by Neptune: further observations of ring arcs *Icarus* **87** 1–39
Nicholson P D, Showalter M R, Dones L, French R G, Larson SM, Lissauer J J, McGhee C A, Seitzer P, Sicardy B and Danielson G E 1996 Observations of Saturn's ring-plane crossings in August and November 1995 *Science* **272** 509–15
Nicholson P D, French R G, Tellestrup E, Cuzzi J N, Harrington J, Matthews K, Perkovic O and Stover R J 2000 Saturn's rings I. Optical depth profiles from the 28 Sgr occultation *Icarus* **145** 474–501
Northrop T B and Connerney J E 1987 A meteorite erosion model and the age of Saturn's rings *Icarus* **70** 124–37
Ockert M E, Cuzzi J N, Porco C C and Johnson T V 1987 Uranian ring photometry: results from Voyager 2 *J. Geophys. Res.* **92** 14696–979
Ockert-Bell M E, Burns J A, Daubar I J, Thomas P C, Veverka J, Belton M J S and Klaasen K P 1999 The structure of Jupiter's ring system as revealed by the Galileo imaging experiment *Icarus* **138** 188–213
Peale S J 1986 Orbital resonances, unusual configurations and exotic rotation states among the planetary satellites *Satellites* ed J A Burns and M S Matthews (Tucson: University of Arizona Press) pp 159–223
Porco C C 1983 Voyager Observations of Saturn's rings *PhD Thesis* California Institute of Technology

Porco C C 1990 Narrow rings: observation and theory *Adv. Space Res.* **10** 221–9
Porco C C 1991 An explanation for Neptune's ring arcs *Science* **253** 995–1001
Porco C C and Goldreich P 1987 Shepherding to the Uranian rings I. Kinematics *Astron. J.* **93** 724–9
Porco C C and Nicholson P D 1987 Eccentric features in Saturn's outer C ring *Icarus* **72** 437–67
Porco C C, Danielson G E, Goldreich P, Holberg J B and Lane A L 1984a Saturn's non-axisymmetric ring edges at $1.95R_S$ and $2.27R_S$ *Icarus* **60** 17–28
Porco C C, Nicholson P D, Borderies N, Goldreich G E, Holberg J B and Lane A L 1984b The eccentric Saturnian ringlets at $1.29R_S$ and $1.45R_S$ *Icarus* **60** 1–16
Porco C C, Cuzzi J N, Esposito L W, Lissauer J J and Nicholson P D 1995 Neptune's rings *Neptune* ed D P Cruikshank (Tucson: University of Arizona Press) pp 703–806
Poulet F, Sicardy B, Nicholson P D, Karkoschka E and Caldwell J 2000 Saturn's ring plane crossings of August and November 1995: a model for the new F ring objects *Icarus* **144** 135–48
Röpke G 1987 *Statistische Mechanik für das Nichtgleichgewicht* (Berlin: VEB Deutscher Verlag der Wissenschaften)
Rosen P A 1989 Waves in Saturn's rings probed by radio occultation *PhD Thesis* Stanford University
Rosen P A, Tyler G L and Marouf E A 1991a Resonance structures in Saturn's rings probed by radio occultation I. Methods and examples *Icarus* **93** 3–24
Rosen P A, Tyler G L, Marouf E A and Lissauer J J 1991b Resonance structures in Saturn's rings probed by radio occultation II. Results and interpretation *Icarus* **93** 25–44
Salo H 1995 Simulations of dense planetary rings III. Self-gravitating identical particles *Icarus* **117** 287–312
Salo H and Hänninen J 1998 Neptune's partial rings: action of Galatea on self-gravitating arc particles *Science* **282** 1102–4
Schaffer L E 1989 The dynamics of dust in planetary magnetospheres *PhD Thesis* Cornell University
Schaffer L E and Burns J A 1987 The dynamics of weakly charged dust: motion through Jupiter's gravitational and magnetic field *J. Geophys. Res.* **92** 2264–80
Schmidt J, Salo H, Spahn F and Petzschmann O 2001 Viscous overstability in Saturn's B-Ring II. Hydrodynamic theory and comparison to simulations *Icarus* **153** 316–31
Showalter M R 1989 Anticipated time variations in (our understanding of) Jupiter's ring system *Time-Variable Phenomena in the Jovian System* ed M J S Belton, R A West and J Rahe NASA SP-494 National Aeronautics and Space Administration
Showalter M R 1991 The visual detection of 1981S13 and its role in the Encke Gap *Nature* **351** 709–13
Showalter M R 1998 Detection of centimeter-sized meteoroid impact events in Saturn's F ring *Science* **282** 1099–102
Showalter M R and Burns J A 1982 A numerical study of Saturn's F-ring *Icarus* **52** 526–44
Showalter M R and Nicholson P D 1990 Saturn's rings through a microscope: particle size constraints from the Voyager PPS scan *Icarus* **87** 285–306
Showalter M R, Burns J A, Cuzzi J N and Pollack J B 1987 Jupiter's ring system: new results on structure and particle properties *Icarus* **69** 458–98
Showalter M R, Cuzzi J N and Larson S M 1991 Structure and properties of Saturn's E ring *Icarus* **94** 451–73
Showalter M R, Pollack J B, Ockert M E, Doyle L R and Dalton J B 1992 A photometric study of Saturn's F ring *Icarus* **100** 394–411
Shu F H 1970 On the density wave theory of galactic spirals *Astrophys. J.* **160** 99–112
Shu F H 1984 Waves in planetary rings *Planetary Rings* ed R Greenberg and A Brahic (Tucson: University of Arizona Press) pp 513–61
Shu F H and Stewart G R 1985 The collisional dynamics of particulate disks *Icarus* **62** 360–383
Shu F H, Yuan C and Lissauer J J 1985a Nonlinear spiral density waves: an inviscid theory *Astrophys. J.* **291** 356–76
Shu F H, Dones L, Lissauer J J, Yuan C and Cuzzi J N 1985b Nonlinear spiral density waves: viscous damping *Astrophys. J.* **299** 542–73
Sicardy B and Lissauer J J 1992 Dynamical models of the arcs in Neptune's 63K ring (1989N1R) *Adv. Space Res.* **12** 97–111
Sicardy B, Roddier C, Roddier F, Perrozzi E, Graves J E, Guyon O and Northcott M J 1999 Images of Neptune's ring arcs obtained by a ground-based telescope *Nature* **400** 731–33
Smith B A *et al* 1982 A new look at the Saturn system: the Voyager 2 images *Science* **215** 504–37
Smith B A *et al* 1986 Voyager 2 in the Uranian system: imaging science results *Science* **233** 43–64
Smith B A *et al* 1989 Voyager 2 at Neptune: imaging science results *Science* **246** 1422–49
Smith W H, McCord T B and Macy W 1981 High-spectral-resolution imagery of Saturn *Icarus* **46** 256–62
Soter S 1971 *The Dust Belts of Mars CRSR Report* 462 Cornell University
Stevenson D J, Harris A W and Lunine J I 1986 Origins of satellites *Satellites* ed J A Burns and M S Matthews (Tucson: University of Arizona Press) pp 39–88

Stewart G R, Lin D N C and Bodenheimer P 1984 Collision-induced transport processes in planetary rings *Planetary Rings* ed R Greenberg and A Brahic (Tucson: University of Arizona Press) pp 447–512

Tagger M, Henriksen R N and Pellat R 1991 On the nature of spokes in Saturn's rings *Icarus* **91** 297–314

Thomas P C 1989 The shapes of small satellites *Icarus* **77** 248–74

Throop H B and Esposito L W 1998 G ring particle sizes derived from ring plane crossing observations *Icarus* **131** 152–66

Throop H B, Esposito L W and Brooks S 2002 Origin and age of the Jovian main ring, in preparation

Tyler G L, Sweenam D N, Anderson J D, Campbell J K, Eshleman V R, Hinson D P, Levy G S, Lindal G F, Marouf E A and Simpson R A 1986 Voyager 2 radio science observations of the Uranian system: atmospheres, rings, satellites *Science* **233** 79–84

van Helden A 1984 Rings in astronomy and cosmology 1600–1900 *Planetary Rings* ed R Greenberg and A Brahic (Tucson: University of Arizona Press) pp 12–24

Ward W R 1981 On the radial structure of Saturn's ring *Geophys. Res. Lett.* **8** 641–3

Warwick J W *et al* 1986 Voyager-2 radio observations of Uranus *Science* **233** 102–6

Weidenschilling S J, Chapman C R, Davis D R and Greenberg R 1984 Ring particles: collisional interactions and physical nature *Planetary Rings* ed R Greenberg and A Brahic (Tucson: University of Arizona Press) pp 367–415

Wisdom J and Tremain S 1988 Local simulations of planetary rings *Astron. J.* **95** 925–40

Zebker H A, Marouf E A and Tyler G L 1985 Saturn's rings: particle size distributions for thin layer models *Icarus* **64** 531–48